arXiv:1205.5765v1 [astro-ph.EP] 25 May 2012

A shared frequency set between the historical mid-latitude aurora records and the global surface temperature

Nicola Scafetta [1]

[1]*ACRIM (Active Cavity Radiometer Solar Irradiance Monitor Lab) & Duke University, Durham, NC 27708, USA.*

Abstract

Herein we show that the historical records of mid-latitude auroras from 1700 to 1966 present oscillations with periods of about 9, 10-11, 20-21, 30 and 60 years. The same frequencies are found in proxy and instrumental global surface temperature records since 1650 and 1850, respectively and in several planetary and solar records. Thus, the aurora records reveal a physical link between climate change and astronomical oscillations. Likely, there exists a modulation of the cosmic ray flux reaching the Earth and/or of the electric properties of the ionosphere. The latter, in turn, have the potentiality of modulating the global cloud cover that ultimately drives the climate oscillations through albedo oscillations. In particular, a quasi 60-year large cycle is quite evident since 1650 in all climate and astronomical records herein studied, which also include an historical record of meteorite fall in China from 619 to 1943. These findings support the thesis that climate oscillations have an astronomical origin. We show that a harmonic constituent model based on the major astronomical frequencies revealed in the aurora records is able to forecast with a reasonable accuracy the decadal and multidecadal temperature oscillations from 1950 to 2010 using the temperature data before 1950, and vice versa. The existence of a natural 60-year modulation of the global surface temperature induced by astronomical mechanisms, by alone, would imply that at least 60-70% of the warming observed since 1970 has been naturally induced. Moreover, the climate may stay approximately stable during the next decades because the 60-year cycle has entered in its cooling phase.

Please, cite this article as: Scafetta N., 2012. A shared frequency set between the historical mid-latitude aurora records and the global surface temperature. Journal of Atmospheric and Solar-Terrestrial Physics 74, 145-163. DOI: 10.1016/j.jastp.2011.10.013. http://dx.doi.org/10.1016/j.jastp.2011.10.013

Keywords: aurora cycles, planetary motion, solar variability, climate

---

1. Introduction

Since ancient times people have claimed that climate and weather changes are related to cyclical astronomical phenomena linked to the orbits of the Sun, the Moon and the planets (Ptolemy, 2nd century; Maʿšar, 886; Kepler, 1606; Swerdlow, 1998; Iyengar, 2009). Because of this conviction the ancient astronomers developed calendars that contain several cycles (Aslaksen, 1999) as well as the well-known annual cycle. During the last 70 years, numerous scientific evidences appear to have corroborated that ancient conviction. For example, Milankovic (1941) theorized that variations in eccentricity, axial tilt and precession of the orbit of the Earth determine climate patterns such as the 100,000 year ice age cycles of the Quaternary glaciation. Milankovitch's theory fits the data very well, over the past million years, in particular if the temporal rate of change of global ice volume is considered (Roe et al., 2006). More recently, a number of authors (Shaviv, 2003; Shaviv and Veizer, 2003; Svensmark, 2007) have shown that the cosmic-ray flux records well correlate with the warm and ice periods of the Phanerozoic during the last 600 million years: in this case the cosmic-ray flux oscillations are believed to be due to the changing galactic environment of the solar system, as it crosses the spiral arms of the Milky Way. Over millennial and secular time scales several authors have found that changes in sunspot number and cosmogenic isotope productions well correlate with climate changes (Eddy, 1976; Sonett and Suess, 1984; Hoyt and Schatten, 1997; White et al., 1997; van Loon and Labitzke, 2000; Bond et al., 2001; Kerr, 2001; Douglass and Clader, 2002; Kirkby, 2007; Scafetta and West, 2005, 2007, 2008; Shaviv, 2008; Raspopov et al., 2008; Eichler et al., 2009; Soon, 2009; Meehl et al., 2009; Scafetta, 2009). Moreover, instrumental global surface records since 1850 appear to be characterized by a set of frequencies that can be associated to the Moon (9.1-year period) and to the motion of the Sun relative to the barycenter of the solar system (about 10.5, 20, 30 and 60 year periods)(Scafetta, 2010a,b).

In this paper, we study the historical mid-latitude aurora records since 1700 (Křivský and Pejml, 1988; Silverman, 1992) and show that these records share the same set of frequencies that characterize the climate system as well as the natural oscillations of the solar system. This finding reveals the existence of a clearer physical mechanism, missing in our previous study (Scafetta, 2010b), that could link the astronomical cycles to climate oscillations. The major implication of this paper is that there exists an astronomical harmonic modulation of the electric properties of the Earth's atmosphere that modulates cloud cover and, therefore, the terrestrial albedo (Svensmark, 1998, 2007; Svensmark et al., 2009; Kirkby, 2007; Tinsley, 2008).

This research would also support the development of a novel astronomically-based theory of climate change that may credibly compete and likely substitute the current mainstream anthropogenic global warming theory (AGWT) advocated by the IPCC (2007). In fact, the AGWT advocates claim that astronomical forcings of the climate are almost negligible and that the climate variations are induced by some still poorly understood and modeled *internal chaotic dynamics* of the climate system, and by trends in greenhouse gases (GHG) (mostly CO_2 and CH_4) and aerosol records. More precisely, global surface temperature has risen (Brohan et al., 2006) by about 0.8 ^oC and 0.5 ^oC since 1900 and 1970, respectively. The IPCC (2007) and other researchers (Lean and Rind, 2008) have claimed that more than 90% of the observed warming since 1900 and practically 100% of the observed warming since 1970 have had an anthropogenic cause. While Lean and Rind's methodology that the climate responds linearly with the forcings can be easily questioned by noting that the heat capacity of the Earth is not zero (Scafetta, 2009), the IPCC claims derive from figures 9.5 and 9.6 in the IPCC report (AR4-WG1, 2007) showing, by means of professional climate general circulation models (GCMs), that natural forcings alone (volcano and solar irradiance) would have caused a cooling since 1970: thus, the observed post-1970 warming has been interpreted as being induced by human activity alone. However, the very large uncertainty in the aerosol forcings and of the climate sensitivity to GHG changes (IPCC, 2007; Knutti and Hegerl, 2008; Rockström et al., 2009; Lindzen and Choi, 2011; Spencer and Braswell, 2011), and the current very poor modeling of the water vapor feedback (Solomon et al., 2010), of the cloud system (Lauer et al., 2010), of the ocean dynamics and of the biosphere question the robustness of the current GCMs for properly interpreting and reconstructing the real climate(Idso and Singer, 2009).

On the contrary, if the climate system is mostly characterized by a specific set of harmonics, it may be possible to partially reconstruct and forecast it in the same way in which ocean tides are currently predicted, that is, by means of harmonic constituent models based on astronomical cycles (Thomson, 1881; Fischer, 1912; Doodson, 1921). A harmonic constituent model is just a superposition of several harmonic terms of the type

$$F(t) = A_0 + \sum_{i=1}^{N} A_i \cos(\omega_i t + \phi_i). \tag{1}$$

The frequencies ω_i are deduced from astronomical theories. The amplitude A_i and the phase ϕ_i of each harmonic are empirically determined using regression on an adequate sample of observations, and then the model is used to forecast future scenarios. Currently, in most US costal locations tidal forecast is made with 35-40 harmonic constituents (Ehret, 2008).

In the following, we show that typical energy balance models and general circulation models can be mathematically reduced to harmonic models in first approximation, and propose that the climate oscillations too can be approximately reconstructed and forecasted by using a planetary harmonic constituent model philosophically equivalent to Eq. 1 based on astronomical cycles.

2. A possible link between mid-latitude auroras and the cloud system

In this paper, we postulate that the annual frequency occurrence of mid-latitude aurora events is a measure of the level of electrification of the global ionosphere, which is mostly regulated by incoming cosmic ray flux variations (Kirkby, 2007; Svensmark, 2007). When the ionosphere is highly ionized by cosmic rays, large auroras would more likely form at the mid-latitudes. This phenomenon would occur because when the upper atmosphere is highly ionized, it would also be electrically quite sensitive to large solar wind particle fluxes and favor the formation of extended mid-latitude auroras. In fact, higher ionization of the atmosphere would mostly occur when the magnetosphere is weaker and cosmic ray as well as solar wind particles, can more easily reach the mid-latitudes. Then, the level of atmospheric ionization and of the global electric circuit of the atmosphere should regulate the cloud system (Kirkby, 2007; Svensmark, 2007; Tinsley, 2008). If the above theory is correct, the frequencies of the mid-latitude aurora records should be present in the climate records too.

Indeed, cloud-related climatic effects can largely dominate other mechanisms such as CO_2 and CH_4 GHG forcing (Kirkby, 2007; Svensmark, 2007). For example, in the past billion years the Earth experienced severe glaciations despite the fact that the CO_2 concentration was at least 10 times higher than today (4000-6000 ppmv against the actual 390 ppmv) (Hayden, 2007). In addition to major continental drifts and other geological events (Courtillot and Renne, 2003), it has also been argued that the high cosmic ray incoming flux that occurred during known major glaciations could have increased the cloudiness of the Earth causing a global cooling (Shaviv, 2003, 2008; Shaviv and Veizer, 2003; Svensmark, 2007).

The cloud system controls a large part of the terrestrial albedo and regulates the amount of total solar irradiance reaching the Earth's surface. The solar irradiance reaching the Earth's surface warms the ocean and the land. A small astronomical modulation of the terrestrial albedo through the cloud system can greatly increase the climate sensitivity to solar forcing (Shaviv, 2008; Scafetta, 2009). Evidently, if the current GCMs are missing an important forcing of the cloud system, they would poorly reconstruct and, potentially, severely misinterpret climate variations at multiple temporal scales. Indeed, a correlation between galactic cosmic ray fluxes and high-altitude, mid-altitude and low clouds have been found (Svensmark, 2007; Rohs et al., 2010; Laken et al., 2010).

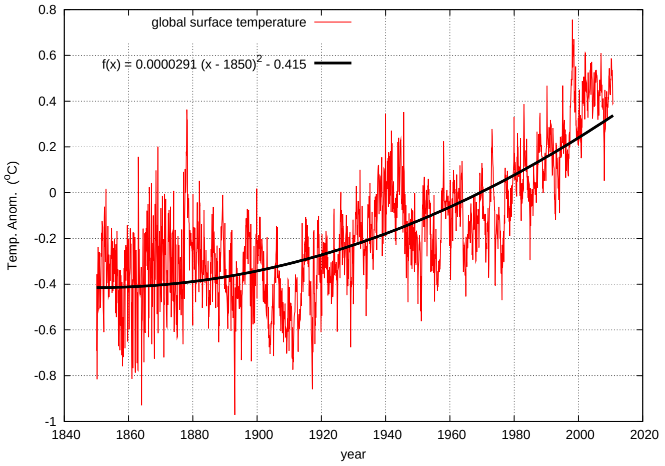

Figure 1: Global surface temperature anomaly (Brohan et al., 2006). The figure also shows the quadratic fit upward trend of the temperature (black).

3. A 60-year cycle in mid-latitude aurora and climate records

Figure 1 shows the global surface temperature (HadCRUT3) (Brohan et al., 2006) from 1850 to 2010 (monthly sampled). Global surface temperature records (land, ocean, north hemisphere, south hemisphere) have been found to be characterized by a clear and large quasi 60-year cyclical modulation (Scafetta, 2010b). In fact, the following 30-year trends are evident in the record: 1850-1880, warming; 1880-1910, cooling; 1910-1940, warming; 1940-1970, cooling; 1970-2000, warming; and a small cooling since 2000 that may last until 2030-2040.

Figure 2A shows the global surface temperature record detrended of its upward trend and smoothed with a 8-year moving average that highlights its 60-year cyclical modulation with a peak-to-trough amplitude of about 0.3-0.4 ^oC.

Figure 2B shows the annual frequencies of mid-latitude auroras obtained from the supplement of the catalogue of mid-latitude auroras <55N from 1700 to 1900. This record contains the historical aurora observations reported mostly in central Europe since 1000 AD (Křivský and Pejml, 1988). Before 1700, the record is largely incomplete and the data are not depicted in the figure. Figure 2B also depicts the catalog of the aurora observations in the Faroes Islands from 1872 to 1966. Despite the fact that the Faroes' record refers to a northern region (62N), Silverman (1992) noted that it appears to have physical properties compatible with the Krivsky and Pejml's record. So, it may be reasonable to combine the two catalogs covering 266 years from 1700 to 1966. The present author does not know why these two records stop in 1900 and 1966 respectively. Aurora events surely have be collected but not with the same naked eye methodologies used in the past. The most recent electronically based records could show technical heterogeneities with the historical ones such that the old and recent records cannot be simply combined. The aurora records are flipped up-down and superimposed to the same 60-year periodic sinusoidal function depicting the 60-year temperature cycles in Figure 2A. Mid-latitude auroras are more likely to occur during cooler multi-decadal periods.

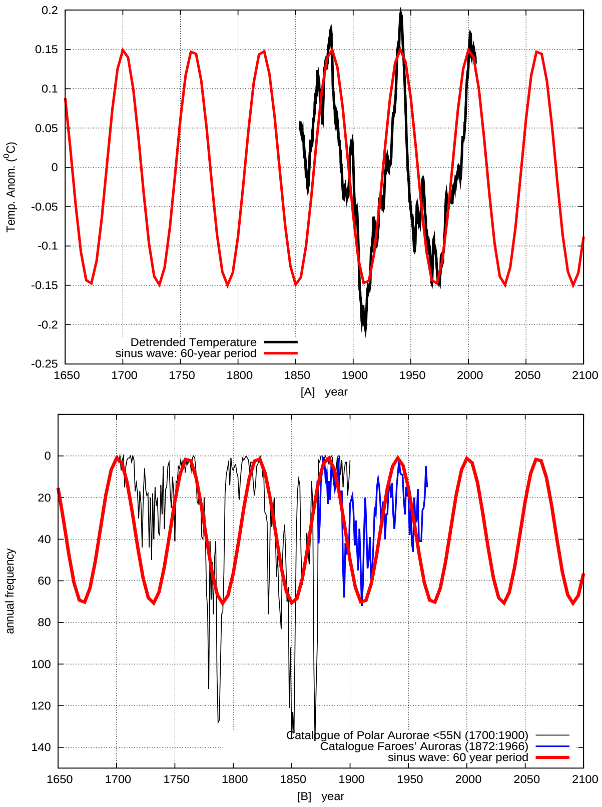

Figure 2: [A] The 60-year cyclical modulation of the global surface temperature obtained by detrending this record of its upward trend shown in Figure 1. The temperature record has been filtered with a 8-year moving average. Note that detrending a linear or parabolic trend does not significantly deform a 60-year wave on a 160-year record, which contains about 2.5 of these cycles, because first and second order polynomials are sufficiently orthogonal to a record containing at least two full cycles. On the contrary, detrending higher order polynomials would deform a 60-year modulation on a 160-year record and would be inappropriate. [B] Aurora records from the "Catalogue of Polar Aurora <55N in the Period 1000-1900" from 1700 to 1900 (Křivský and Pejml, 1988). Figure 2B also depicts the catalog referring to the aurora observations from the Faroes Islands from 1872 to 1966. Both temperature and aurora records show a synchronized 60-year cyclical modulation as proven by the fact that the 60-year periodic harmonic function superimposed to both records is the same.

An approximate 60-year modulation in the aurora record from 1000 to 1900 has been observed by Charvátová-Jakubcová et al. (1988), once that the original record before 1700 is adjusted with what is there called a "civilization" factor coefficient. Komitov (2009) also found a correspondent quasi 60-year cycle in both aurora and Greenland and Antarctic ^{10}Be concentration records during the period 1700-1900. Periodic patterns and long-term variations in the aurora records have been observed for centuries since the work by de Mairan (1733). De Mairan found several reprises and returns in the aurora activity. Siscoe (1980) summarized a number of the studies that searched for periodicities in aurora occurrence. For example, in 1831 Hansteen inferred a period of 95 years; Olmsted (1856) found distinctive evidences for

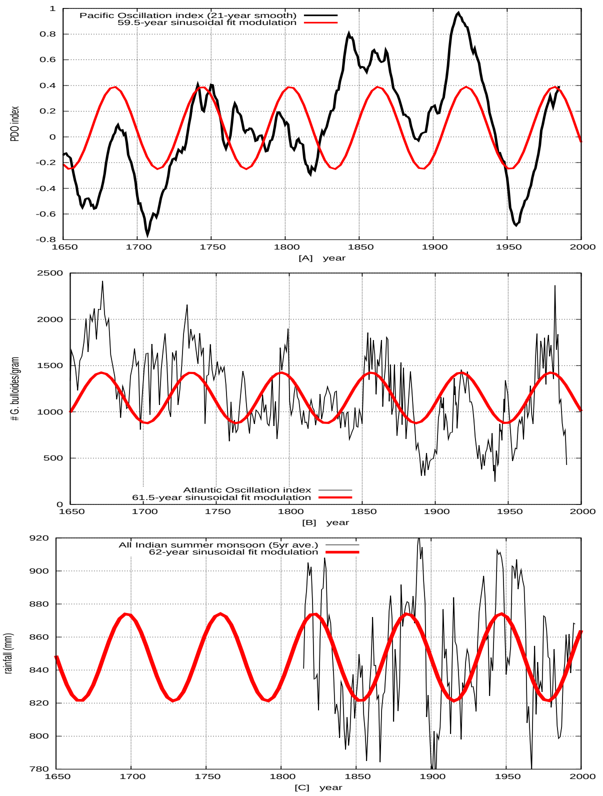

Figure 3: [A] Twenty-year moving average of the tree-ring chronologies from Pinus Flexilis in California and Albertain: this record is used as a proxy for reconstructing the Pacific Decadal Oscillation (MacDonald and Case, 2005). [B] Record of G. Bulloides abundance variations (1-mm intervals) from 1650 to 1990 A.D. (black line) (Black et al., 1999); this is a proxy for the Atlantic variability since 1650. [C] Five-year running average of the Indian summer monsoon rainfall from 1813 to 1998 (Agnihotri and Dutta, 2003). All three records show clear 60-year cyclical modulations that are (positively or negatively) well correlated to the 60-year cycles of the global surface temperature and the aurora records. The records are best fit with sinusoidal functions that give a statistical error about the 60-year period of ±4 years.

60 to 65 years as the intervals between great auroras; and Wolf and Fritz preferred a period of about 55 years. Another work also indicated periods in the region of 80-90 years (Feynman and Fougere, 1984), and even large periods as long as 200 or 400 years. Large cycles with periods of about 60, 80-90 years and longer bi- and multi-secular cycles are the most commonly reported. These frequencies correspond to the well-known Gleissberg and Suess solar cycle frequency bands (Suess, 1980; Křivský and Pejml, 1988; Ogurtsov et al., 2002).

As already discussed in Scafetta (2010a,b), quasi 60-year cycles are found in several climatic from several regions of the Earth (Klyashtorin, 2001; Klyashtorin and Lyubushin, 2007; Klyashtorin et al., 2009; Le Mouël et al., 2008; Camuffo et al., 2010; Agnihotri et al., 2002; Agnihotri and Dutta, 2003; Sinha et al., 2005; Goswami et al., 2006; Yadava and Ramesh, 2007; Mazzarella and Scafetta, 2011; Jevrejeva et al., 2008) and astronomical/solar records (Yu et al., 1983; Patterson et al., 2004; Ogurtsov et al., 2002; Roberts et al., 2007). These results clearly suggest the existence in the climate of a natural 60-year cycle synchronized to a correspondent solar/astronomical cycle. For example, Figure 3 depicts three multi-secular climate records from three independent regions of the globe showing multiple quasi-60 year large oscillations since 1650. Figure 3A depicts a record obtained from the tree-ring chronologies from Pinus Flexilis in California and Albertain: the best sinusoidal fit gives a period of $T = 61.5 \pm 4$ years. This record is used as a proxy for reconstructing the Pacific Decadal Oscillation (MacDonald and Case, 2005). Figure 3B depicts the G. Bulloides abundance variation record found in the Cariaco Basis sediments in the Caribbean sea since 1650 (Black et al., 1999): the best sinusoidal regression fit gives a period of $T = 59.5 \pm 4$ years: a quasi-60 year cycle has been found in the Caribbean sea for millennia during the entire Holocene (Knudsen et al., 1988). This record is an indicator of the trade wind strength in the tropical Atlantic Ocean and of the North Atlantic Ocean atmosphere variability. Periods of high G. Bulloides abundance correlate well with periods of reduced solar output (the well-known Oort, Wolf, Spörer, Maunder, Dalton minima): a fact that suggests that these cycles are solar induced (Black et al., 1999). Figure 3C depicts the Indian summer monsoon rainfall record from 1813 to 1998 years that also shows prominent quasi 60-year cycles. The Indian summer monsoon rainfall record, together with east equatorial and Chinese monsoons, clearly manifest a solar variability signature for several centuries (Agnihotri and Dutta, 2003): the best sinusoidal fit of the Indian monsoon rainfall record gives a period of $T = 62 \pm 4$ years. The cycles depicted in Figures 2 and 3 are well synchronized to the quasi 60-year modulation of the global temperature observed since 1850.

Consequently, the very good correspondence between the two 60-year periods 1880-1940 and 1940-2000, which are observed in all (North and South, Ocean and Land) global surface temperature records (Scafetta, 2010a,b), is unlikely just a coincidental red-noise pattern. With a high confidence level, a natural 60-year periodic modulation exists in the climate system because these cycles are observed in a large number of natural multi-secular records although this cycle may not appear always evident because of errors in the data and because of other superimposed patterns of different physical origin (for example, volcano effects) and other natural cycles that could induce interference patterns.

4. Spectral analysis of aurora and climate data, and joint power statistical tests

To determine whether faster cycles are equally common in the aurora and temperature records we analyze the global surface temperature and the auroras records by using the maximum entropy method (Ghil et al., 2002) because with a proper high number of *poles* this technique resolves the very low frequency band of the spectrum much better than Fourier or periodogram based techniques (Priestly et al., 2001). Note that in our case MEM needs to be used with a very large number of poles (up to half of the length N of the record) because we are interested in resolving the very low frequency range of the spectrum

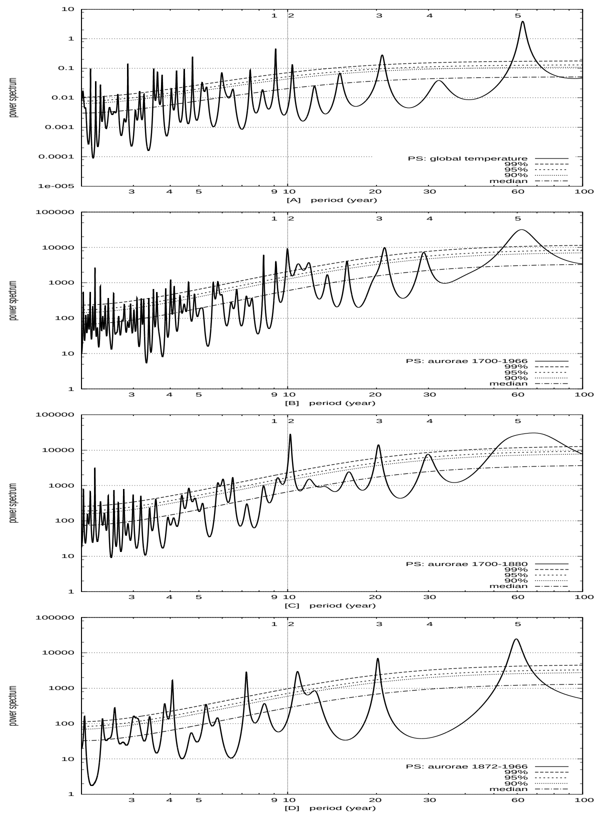

Figure 4: [A] Power spectrum of the global surface temperature [A], which covers the period 1850-2010. [B,C,D] power spectra of three auroras records, which cover the periods 1700-1966, 1700-1880 and 1872-1966 respectively. The numbers #1, #2, #3, #4 and #5 indicate the periods at about 9, 10-11, 20, 30 and 60 years. These peaks are statistically significant against red-noise background tests at different confidence levels (median, % 90, %95, %99), which are indicated with the dot lines.

where the dacadal and multidecadal periodicities are located, as simple computer experiments with synthetic harmonic records would easily prove. A number of poles between N/5 and N/2 (at most) is correct in most cases (Ulrych and Bishop, 1975; Courtillot et al., 1977).

Figure 4A shows the power spectrum of the temperature that covers the period 1850-2009. This curve corresponds to those analyzed in Scafetta (2010b), where additional alternative statistical tests to check the robustness of the results are conducted. Four major decadal and multidecadal cycles are seen at about 9, 10-11, 20-21 and 60-year periods. These cycles are indicated with the number #1, #2, #3 and #5. With the exception of the smaller peak #4 (about 30 years), which may not be significant, all other four frequencies have a 99% confidence against red noise background. Faster cycles or less important cycles are not studied here. Traditional periodogram analysis (not reported in this figure) produces the same major four peaks detected by MEM, but with a larger uncertainty, and confirms that the global surface temperature is characterized by at least the above four major frequency peaks.

Figure 4B shows the power spectrum of the superposition of the catalogues of mid-latitude auroras merged with the Faroes' auroras: this combined record covers the period 1700-1966. Again, five peaks cycles are clearly seen at about 9, 10-11, 20-21, 30 and 60 years. Figure 4C shows the power spectrum of a portion of the catalogue of mid-latitude aurora covering the period 1700-1880, which presents a minimum overlap with the temperature data and with the Faroes' catalog. Again, five peaks are seen at about 9, 10-11, 20-21, 30 and 60 years. Figure 4D shows the power spectrum of the Faroes' catalog that covers the period 1872-1966. In this case, only 3 cycles are clearly seen: cycle #2 (10-11 years); cycle #3 (20-21 years); and cycle #5 (about 60 years). Note that cycle #1 (about 9 years) is not as strong as the one found in the temperature record: we will discuss this finding later.

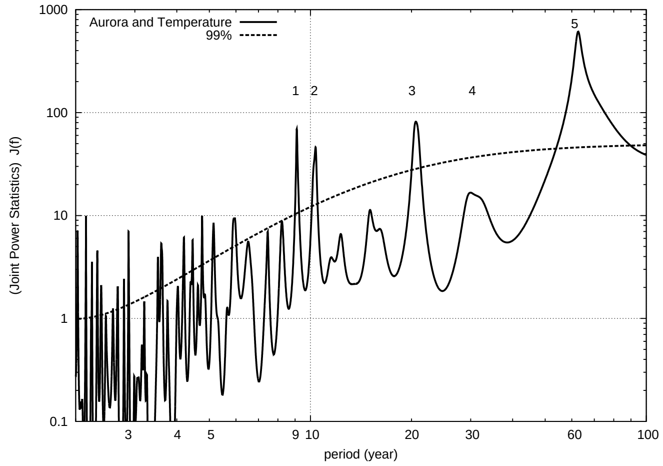

Figure 5: Joint power statistics (Sturrock et al., 2005) between the power spectra of the 1850-2010 global temperature (Figure 4A) and the 1700-1900 aurora record (Figure 4C). The joint peaks at periods of about 9, 10.5, 20 and 60 years are evident and have a 99% confidence level against red-noise background.

Table 1 reports the measured five periods and their average values. The frequencies of the temperature and of the AAR columns are compatible within their error of measure. For the 5 period couples reported in Table 1, the reduced χ^2 is $\chi_o^2 = 0.18$ with 5 degrees of freedom and the coherence probability is $P_5(\chi^2 \geq \chi_o^2) > 96\%$.

Figure 5 further supports the result that the aurora records and the global temperature record share a similar set of frequency. In this case, we use the joint power statistic function (Sturrock et al., 2005) which confirms that the aurora record and the global temperature record share a common set of major cycles at about 9, 10.5, 20, and 60-year periods (cycles #1, #2, #3 and #5) with a 99% confidence. If two power spectra share a compatible frequency peak, also their joint power statistic function, which is approximately given by $\sqrt{S_1(f) * S_2(f)}$, would show a significant peak at the same frequency. Other common cycles may be present as well, but they are less evident.

5. A possible astronomical planetary origin of the aurora and temperature oscillations

The observed aurora and climate cycles suggests that the solar system planetary orbital dynamics may be their first physical cause. Indeed, some studies (Wolf, 1859; Schuster, 1911; Bendandi, 1931; Jose, 1965; Fairbridge and Shirley, 1987; Landscheidt, 1988, 1999; Charvátová, 1990, 2000, 2009; Charvátová and Střeštík, 2004; Grandpierre, 1996; Mackey, 2007; Hung, 2007; Wilson et al., 2008; Sidorenkov and Wilson, 2009; Perryman and Schulze-Hartung, 2010) have suggested that solar variation can be partially driven by the planets through gravitational spin-orbit coupling mechanisms and gravitational tides.

A full theory that would physically explain how the solar wobbling or the planetary tides may influence solar activity has not been fully developed yet. However, preliminary studies suggest that planetary gravity may increase nuclear rate (Grandpierre, 1996; Wolff and Patrone, 2010) by favoring the movement of fresh fuel into the solar core. The proposed mechanisms would likely produce the major frequencies herein discussed because it is based on the study of the wobbling of Sun around the solar system barycenter as done in Scafetta (2010b).

Moreover, solar wobbling could be physically relevant relative to the incoming cosmic ray flux. In fact, because the inner part of the solar system is almost gravitationally locked to the Sun, and the Earth's orbit too wobbles around the solar system's barycenter almost in the same way as the Sun does. Indeed, an observer from the Earth does not see the solar wobbling while an observer external to the solar system would see the Earth's orbit wobbling almost in the same way as the Sun does. Thus, relative to the Sun or to the Earth's orbit, the incoming cosmic ray flux is wobbling with the same frequencies found in the solar barycentric motion (Scafetta, 2010b).

The major planetary resonances of the solar system related to Jupiter and Saturn are the following: Jupiter's sidereal period 11.862 years; Saturn's sidereal period 29.457 years; the opposition-synodic period of Jupiter and Saturn (9.93 year), which oscillates between 9.5 and 10.5 years due to the eccentricity of their orbits; about 19.84 years, the synodic period of Jupiter and Saturn; about 59.6 years, the repetition of the combined orbits of Jupiter and Saturn; and a spring tidal beat frequency (~61 year). Moreover, there is the 11-year Schwabe solar cycle and the 22-year Hale magnetic solar cycle which perhaps are indirectly associated to the two major Jupiter/Saturn tides because the 11-year cycle appears constrained between the 9.3-year spring Jupiter/Saturn tide and the 11.8-year Jupiter tide Wilson (1987). Thus, three major solar and solar system oscillations should be expected at periods of about 10-11, 20-22 and 59-63 years. Many other resonance frequencies related to all planets have been found in the Suns motion (Bucha et al., 1985; Charvátová-Jakubcová et al., 1988), but they are not discussed here.

An additional large 9.1-year temperature cycle does not appear among the planetary resonances and Scafetta (2010b) found that it may be a solar/lunar tidal cycle. In fact, a 9.1-year periodicity is between the period of the recession of the line of lunar apsides, about 8.85 years, and half of the period of precession of the luni-solar nodes, about 9.3 years (the luni-solar nodal period is 18.6 years). The 9.1-year cycle is also about half of the 18.03-year Saros eclipse cycle. Note that every almost 9 tropical years the Sun, the Earth and the Moon are aligned at the same angle relative to the Earth's surface. Because two opposite tides are simultaneously present, the two alignments Sun-Moon-Earth and Sun-Earth-Moon are physically equivalent. Consequently, a quasi 18-year astronomical solar/lunar cycle is associated to a quasi 9-year tidal cycle dynamics.

The results depicted in Figures 4B, 4C and 4D suggest that the aurora events are synchronized to the above astronomical periodicities. About the two decadal cycle in the climate records, several studies have attempted to interpret it either as a lunar influence on climate via the 18.6-year luni-solar nodal or the nutation cycle, or as an influence of the 22-year Hale solar magnetic cycle (Currie, 1984; Keeling and Whorf, 2000; Camuffo, 2001; McKinnell and Crawford, 2007; Munk and Bills, 2007; Hoyt and Schatten, 1997). However, on a global scale the most prominent bi-decadal cycle has a period of about 20-21 years as shown above in Figures 4 and 5, while a distinct 18.6 year lunar cycle or a 22-year solar cycle are not clearly visible in the adopted global temperature records. Perhaps, a 18.6-year nutation cycle may become particularly significant only in some regions, such as the polar ones. Because the global data herein analyzed appear to show a quasi 20-21 year cycle more than a sharp 18.6 or a 22-year cycle, we claim that a quasi 20-21 year cycle is what may characterizes the well known bi-decadal climatic cycle (Scafetta, 2010b).

6. Further analysis of Jupiter and Saturn's orbital dynamics and of their induced solar system cycles

Herein we further analyze how the orbital eccentricities and the periods of Jupiter and Saturn can produce major 10, 20 and 60-year oscillations in the solar system. Figure 6 shows the dates of all conjunctions of Jupiter and Saturn occurred from 1650 to 2010 relative to the Sun. The orbital data are obtained using the NASA Jet Propulsion Laboratory Developmental Ephemeris. The angular separation between Jupiter and Saturn relative to the Sun at the conjunction day is of the order of 1^o, or below. Table 2 reports the dates, the heliocentric coordinates and the distance from the Sun of the conjunctions of Jupiter and Saturn. The coordinates are chosen to be the right ascension and declination, which refer to the equatorial plane of the Earth. Thus, the declination measures the direction of the gravitational and magnetic forces of Jupiter and Saturn relative to the daily average orientation of the terrestrial magnetosphere. The figure shows that the conjunctions since 1650 can be separated into three groups. A conjunction in the Group I is followed by a conjunction in the Group II at an angle of about $360^o * 19.86/29.46 = 242.7^o$ after about 20 years, which is followed by a conjunction in the Group III again at about 242.7^o, after about 20 years. Every 3rd alignment (about 60 years) is about 8.1 degrees of the original starting point: the configuration repeats about every 900 years. A similar diagram

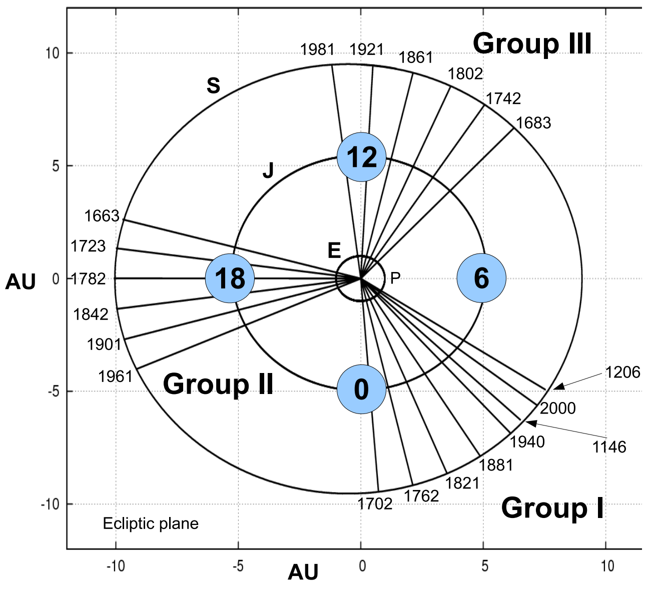

Figure 6: Dates and positions of the conjunctions between Jupiter and Saturn from 1650 to 2010, as reported in Table 2. The figure depicts the orbits of the Earth (E), of Jupiter (J) and of Saturn (S). 'P' is the position of the perihelion of the Earth. The figure emphasizes the tri-synodic cycle of Jupiter and Saturn. It takes about 60 years for Jupiter and Saturn to reach the same relative alignment around the sun. Two J/S conjunctions occurred in 1146 and 1206 are added. The latter two J/S conjunctions reveal a 800-850 year cycle in the J/S conjunction circulation as seen from the Earth and noted by Kepler who was using the tropical orbital period of the planets.

was prepared by Kepler (1606) to interpret the Star of Betlehem as a J/S conjunction (Kemp, 2009), but Kepler used the tropical orbital periods that yield an angular separation of about 3 degree: and the configuration would repeat approximately every 800 years, as depicted in Figure 6.

The last column of Table 2 reports the approximate magnitude in Km of the tidal elongation produced by the combined effect of Jupiter and Saturn at 1 AU from the Sun, which is the Sun-Earth average distance. The tabulated spring tidal elongation values at 1 AU from the Sun are calculated by using the following approximated formula (Taylor, 2005):

$$a_+ - a_- = \frac{3}{2}\frac{M_J}{M_{Su}}\frac{R^4_{SuE}}{R^3_{SuJ}} + \frac{3}{2}\frac{M_S}{M_{Su}}\frac{R^4_{SuE}}{R^3_{SuS}}, \tag{2}$$

where: a_+ and a_- are, respectively, the maximum and minimum radius of the equipotential surface spheroid produced by the gravitational field of the Sun plus the tidal potentials of Jupiter and Saturn; $M_{Su} = 333000$, $M_J = 317.9$ and $M_S = 95.18$ are the masses of the Sun, Jupiter and Saturn in Earth's masses; R_{SuJ} and R_{SuS} are the distances of the Sun from Jupiter and Saturn, respectively; and $R_{SuE} = 1$ AU is the average Sun-Earth distance.

Table 2 shows that the tidal elongations at the J/S conjunctions occurring in Group I are significantly larger (about 1800 Km) than those occurring in the other two groups: about 1400 Km and 1600 Km respectively. The results about the tidal elongation indicate that Group I alignments occur when Jupiter and Saturn occupy the closest positions to the Sun and their combined tidal effect is the largest. This returning pattern gives origin to a 60-year physical tidal cycle on the Sun and in the heliosphere in proximity of the Earth's orbit. A similar 60-year periodic pattern would be generated by the magnetic fields of Jupiter and Saturn that influence the heliosphere too.

To show the varying effect of the tidal combination of the J/S synodic cycle and Jupiter eccentricity cycle we observe that: a) the tidal oscillation produced by Jupiter and Saturn orbits at 1 AU have an amplitude of about 224 km and 12.3 Km, respectively, which are calculated as half of the difference between the tidal elongation at the perihelion and at the aphelion; b) J/S synodic cycle produces an average tide amplitude of about 38.4 Km, which is the half amplitude of the average Saturn induced tidal elongation. Jupiter's perihelion occurred on 20/May/1999 ($\tau_1 = 1999.38$), Saturn's perihelion occurred on 27/Jul/2003 ($\tau_2 = 2003.57$) and the J/S conjunction occurred on 23/Jun/2000 ($\tau_3 = 2000.48$). Thus, the average J/S tidal anomaly effect approximately oscillates as

$$\begin{aligned} D(t) \;=\; & 224\cos\left[\frac{2\pi\,(t-\tau_1)}{11.86}\right] + \\ & \left(38.4 + 12.3\cos\left[\frac{2\pi\,(t-\tau_2)}{29.46}\right]\right)\cos\left[\frac{2\pi\,(t-\tau_3)}{9.93}\right], \end{aligned} \tag{3}$$

where it is assumed the superposition of two waves given by the tidal sidereal orbit of Jupiter and the spring tidal oscillation of Jupiter and Saturn.

Figure 7A depicts the function $D(t)$ for the period 1650-2050. The quasi 60-year beat modulation is evident, and it is in good phase with the 60-year modulations observed in Figures 2 and 3. Note, for example, that the function $D(t)$ presents minimum amplitudes during periods of temperature minima (1850-1860, 1900-1920, 1960-1980) and maximum amplitudes during periods of temperature maxima (1870-1890, 1930-1950, 1990-2010).

Figure 7B depicts the speed of Sun relative to the barycenter of the solar system where the 20-year and 60-year modulation of the solar orbit is also evident. Note that the 60-year modulation of the solar speed corresponds exactly to the 60-year modulation of the auroras and of the climate depicted in Figure 2.

The existence of an astronomical 60-year cycle that is influencing the inner part of the solar system is further proven by meteorite fall records, as extensively studied in Yu et al. (1983). It is well known that Jupiter and Saturn can regulate the collision rate of small bodies with the Earth (Bennett et al., 2010). Figure 8 shows our analysis of a number of historically recorded meteorites falls in China from AD 619 to 1943. Although this record may be incomplete and should be corrected by some social parameters, it shows cycles at about 10.5, 30 and 60 year periods. This result would stress the importance of the J/S 60-year cycle in driving a major astronomical oscillation of the solar system. The power spectrum in the insert of

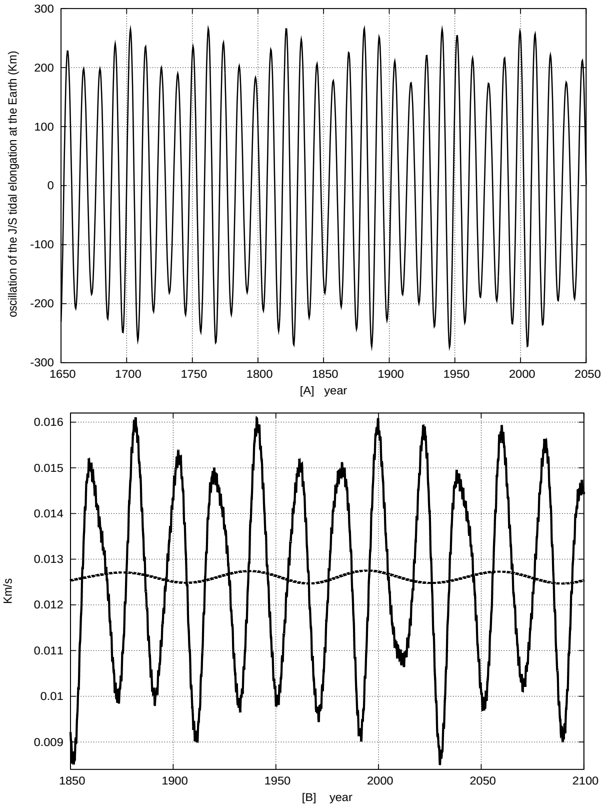

Figure 7: [A] The Jupiter-Saturn tidal anomaly as deduced from Eq. 3 at 1 AU from the Sun. Note the 60-year beat modulation. This 60-year modulation is in good phase with the 61-year cycle of the temperature and of the aurora records since 1700 depicted in Figures 2 and 3: the largest magnitudes correspond to peaks of the 61-year cycles. [B] Figure B depicts the speed of Sun relative to the solar system barycenter (SSSB) (Scafetta, 2010b). The 20-year (solid) and 60-year (dash) oscillation is evident. The dash curve is a moving average filtering. Note that the 60-year modulation observed in both figures corresponds exactly to the 60-year modulation of the auroras and of the climate depicted in Figure 2.

Figure 8 also suggests the astronomical origin of a significant $\sim$10.5-year cycle, which is also found in the temperature record (see Table 1) and in the alignments of the tide-raising planets within ten degrees (Okal and Anderson, 1975; Bucha et al., 1985; Grandpierre, 1996).

Quasi-millennial solar cycles are evident in several cosmogenic isotope productions (Bard et al., 1999; Bond et al., 2001; Kerr, 2001; Steinhilber et al., 2009). Figure 6 shows that the J/S conjunctions in AD 1146 and 1206 occurred approximately at the same position of the conjunction in 2000. Thus, the J/S conjunction line presents a 800-860 year cycle, as Kepler (1606) found where the tropical orbital periods ($P_J = 11.857$ and $P_S = 29.424$) were used. Moreover, the distance of the two planets from the Sun at the conjunction dates presents a quasi 900-year cycle because of their orbital precession, as it is evident by comparing the tidal elongations in 1086 and 2000, which could be obtained using the sidereal orbital periods ($P_J = 11.862$ and $P_S = 29.457$), which are more physical relative to the Sun. The orbital pattern reveals the existence in the solar system of quasi-millennial cycles. Quasi-millennial cycles have been found in solar proxy records [for example see: Hood and Jirikowic (1991); Charvátová (2000); Bond et al. (2001); Kerr (2001); Steinhilber et al. (2009)] and quasi 900-year cycles have been found in the Holocene climate variability (Schulz and Paul, 2002). A quasi-millennial cycle is quite evident in numerous global temperature reconstructions that show a large preindustrial variability. These reconstructions show a distinctive Roman Optimum (0-400 AD), a Medieval Dark Age (400-900 AD), Medieval Warm Period (MWP) (900-1300 AD), a Little Ice Age (LIA) (1400-1800 AD) and a Current Warm Period (CWP) since 1800 (Moberg et al., 2005; Loehle and Mc Culloch, 2008; McShane and Wyner, 2011; Ljungqvist, 2010) and in numerous recent regional records such as from England, Sargasso sea, Japan, Antarctic, Canada, Chile, Indo-pacific region, China, tropical South America, and many more (Lamb, 1965; Parker et al., 1992; Keigwin, 1996; Adhikari and Kumon, 2001; Khim et al., 2002; Huang et al., 2008; Cook et al., 2009; von Gunten et al., 2009; Oppo et al., 2009; Ge et al., 2010; Kellerhals et al., 2010; Mann et al., 2008; Ljungqvist, 2009). However, these quasi-millennial cycles, as well as other secular and multi-secular cycles may be the topic of another work; we only note that the latter temperature reconstructions contradict the *Hockey Stick* temperature graphs (Mann and Jones, 2003) that do not show a significant MWP nor a LIA, but only an unprecedented CWP. The most recent temperature reconstructions would imply the overall solar forcing of the climate has been underestimated by at least a factor of three by traditional energy balance models Scafetta (2010a).

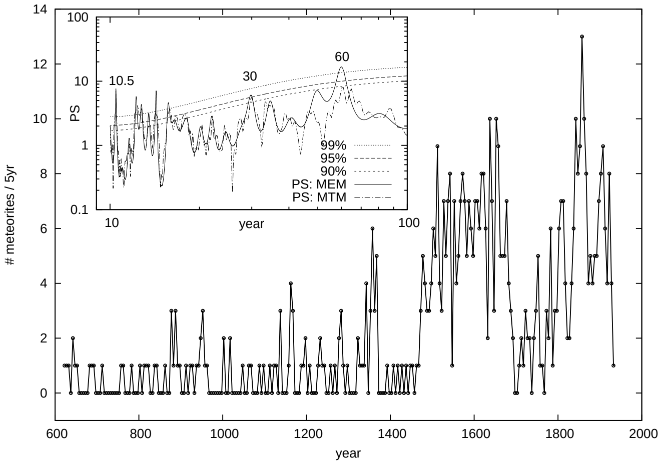

Figure 8: Number of historically recorded meteorite fall in China from AD 619 to 1943 Yu et al. (1983). Note that the gradual multi-secular increase of witnessed meteorite falls is likely due to social parameters effects. In fact, in China, the typography (book-printing) has been known since AD. 1041 while only hand written records are available before, so the records are very scarce in the first millennium in comparison with the greater number of records in the second half of the second millennium. However, this trending should not significantly alter the faster decadal and multidecadal modulation, which should be physical meaningful. The insert shows the power spectrum of the record with the Maximum Entropy Method (50 poles) and the Multi Taper Method. Cycles at 10.5, 30 and 60 years are clearly visible.

7. Cloud cover oscillation as a possible mechanism for climate cycles

Total solar irradiance variations alone are usually claimed to be too small to induce large climate variations (IPCC, 2007). Additional solar related forcings would be necessary to explain climatic variations. Indeed, there may be an additional effect on climate due to ultraviolet modulation of the stratospheric ozone and stratospheric water vapor (Stuber et al., 2001; Solomon et al., 2010), and a modulation of the cloud cover due to cosmic ray flux variation and a variation of the global electric circuit (Shaviv and Veizer, 2003; Svensmark, 2007; Rohs et al., 2010; Laken et al., 2010; Tinsley, 2008).

Variations of the frequency of mid-latitude aurora reasonably reveal electric variations occurring in the terrestrial magnetosphere and ionosphere. Likely, when the upper atmosphere is more ionized, it is more sensitive to solar wind peak activity and mid-latitude aurora events occur more frequently. Therefore, the mid-latitude aurora records can be considered as a proxy of the variation of the atmospheric ionization and, likely, of the atmospheric global electric circuit. As proposed by several authors (Tinsley, 2008; Svensmark, 2007), changes in the global electric circuit can drive changes of cloud formation and cover. A change of cloud cover alters the albedo and can potentially cause a significant climate change. Because auroras oscillated with planetary frequencies the climate would oscillate with the same frequencies and would be almost perfectly synchronized to the 10-11, 20-21 and 60-62 year cycles of the J/S conjunction, tidal and solar cycles, as shown in Scafetta (2010b). Several other cycles are surely present, but we do not discuss them here.

To emphasize the effect that a small variation of the albedo may have on the climate sensitivity to solar changes we can do the following exercise. Let us write:

$$\Delta T \approx \sum_F \Delta T_F \approx \sum_F k_F \, \Delta F, \tag{4}$$

where ΔT_F is the change in temperature caused by a small change of a generic forcing ΔF. The value k_F is the equilibrium climate sensitivity to a small changes in the forcing, as measured by ΔF. In the case of solar irradiance the above equation is substituted with $\Delta T_S \approx k_S \, \Delta F_S$. The same can be done for any other forcings.

By differentiating directly a corrected Stefan-Boltzmann's black-body equation

$$f \, \frac{(1-a)I}{4} = \sigma T^4, \tag{5}$$

we get

$$k_S = \frac{\Delta T}{\Delta I} = \frac{T}{4I} = 0.053 \, K/Wm^{-2} \tag{6}$$

using $I = 1360 \; W/m^2$ as the average total solar irradiance, $a = 0.3$ as the average albedo, $T = 289$ K as the global average temperature of the Earth's surface and $\sigma = 5.67 \times 10^{-8} \; W/m^2K^4$ is the Stefan-Boltzmann's constant. A corrective amplification coefficient $f = 1.65$ is used to approximate the greenhouse effect of the terrestrial atmosphere to let Eq. 5 to give an equilibrium temperature of $T = 289$ K.

The above k_S estimate in Eq. 6 assumes, for example, that the albedo a is constant. Now, let us assume that an increase of the total solar irradiance input of $\Delta I = 1 \; W/m^2$ is accompanied at equilibrium with a decrease of the albedo by just 1% that could be caused also by alternative related solar forcing such as a cosmic ray flux solar modulation. The decrease of the albedo may be due to a decrease of the low cloud cover and other possible factors such as a darkening of the Earth's surface due to a melting of the glaciers and biosphere changes. If we assume that everything else remains constant, the climate sensitivity to total solar irradiance change becomes

$$k_S = \frac{\Delta T}{\Delta I} = \frac{\sqrt[4]{\frac{(1-a*0.99)(I+\Delta I)f}{4\sigma}} - \sqrt[4]{\frac{(1-a)If}{4\sigma}}}{\Delta I} \approx 0.36 \, K/Wm^{-2}, \tag{7}$$

which is seven times larger than the value found in Eq. 6 and would be approximately compatible with the empirical values found in Scafetta (2009). This suggests that even very small solar-induced modulation of the albedo (just a 1 or 2% variation) can greatly amplify the climate sensitivity to solar irradiance changes even by one order of magnitude and could easily induce climatic oscillation of the order of a few tenths of Celsius degree, which would be perfectly compatible with the observations.

There may also be the possibility that the terrestrial albedo is directly modulated by other astronomical mechanisms such as a compression of the Earth's magnetosphere due to tidal forces. Also in this case Eq. (5) would present an albedo that would be a function of time, $a(t)$, and this function would vary with the periods of the astronomical forcing. Even in the eventuality that the incoming total solar irradiance I and the greenhouse feedback coefficient f remain constant, it is easy to prove, using Eq. (7), that a reduction of the albedo by just 1%, for example a decrease from $a = 0.300$ to $a = 0.297$, would cause an increase of the global temperature at equilibrium of about 0.3 K.

The oscillations observed in the aurora records may suggest that the cloud cover oscillates in the same way. Thus, we can assume, in first approximation, an albedo function that changes periodically as

$$a(t) = a_0 + \sum_i a_i \, \cos(\omega_i \, t + \phi_i), \tag{8}$$

where $a_0 \approx 0.3$ is the average terrestrial albedo, ω_i and ϕ_i with $i = 1, 2, 3, \ldots$ are the planetary frequencies and phases, and a_i are the amplitudes of these cyclical fluctuations.

We observe that a significant, although small decadal modulation, of the low cloud cover since 1980, appears synchronized to the decadal solar cycle (Harrison and Stephenson, 2005; Svensmark, 2007; Brown, 2008). Also a careful analysis of a critical study (Sloan and Wolfendale, 2008) would approximately support the theory: their figure 1 shows the low cloud cover anomalies in the polar, intermediate and equatorial regions from 1980 to 2005, and a sufficiently clear decadal cycle,

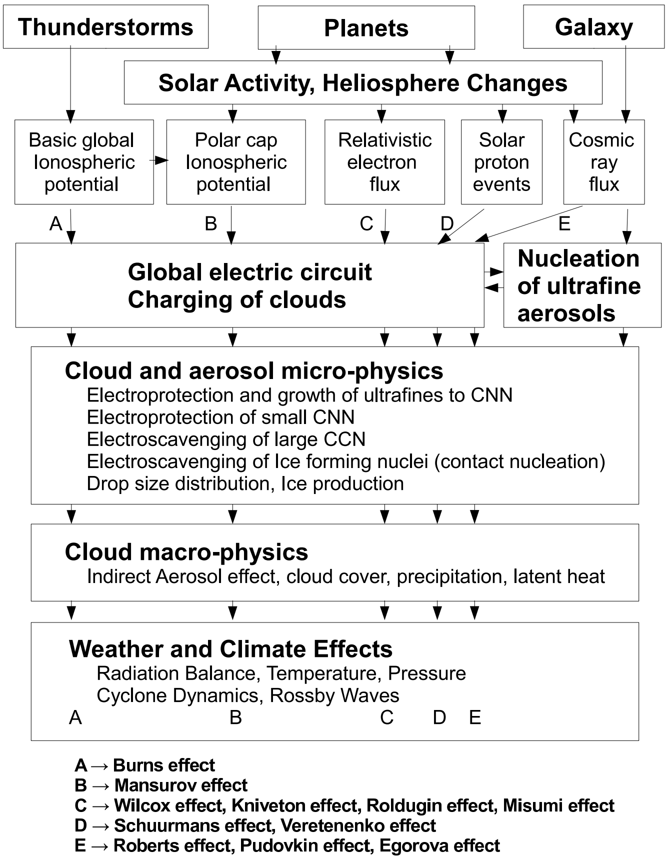
Thunderstorms
Planets
Galaxy
Solar Activity, Heliosphere Changes
Basic global Ionospheric potential
Polar cap Ionospheric potential
Relativistic electron flux
Solar proton events
Cosmic ray flux
A
B
C
D
E
Global electric circuit Charging of clouds
Nucleation of ultrafine aerosols
Cloud and aerosol micro-physics
Electroprotection and growth of ultrafines to CNN
Electroprotection of small CNN
Electroscavenging of large CCN
Electroscavenging of Ice forming nuclei (contact nucleation)
Drop size distribution, Ice production
Cloud macro-physics
Indirect Aerosol effect, cloud cover, precipitation, latent heat
Weather and Climate Effects
Radiation Balance, Temperature, Pressure
Cyclone Dynamics, Rossby Waves
A
B
C
D
E
A → Burns effect
B → Mansurov effect
C → Wilcox effect, Kniveton effect, Roldugin effect, Misumi effect
D → Schuurmans effect, Veretenenko effect
E → Roberts effect, Pudovkin effect, Egorova effect

Figure 9: Connections between weather and climate with thunderstorms, solar activity, and galactic cosmic ray flux, via the global atmospheric electric circuit and cloud and aerosol microphysics. Solar and heliospheric activity is supposed to be partially driven by the gravitational and magnetic fields of the planets, as they move around the Sun. See Tinsley (2008) for more details about the single mechanisms reported in the figure.

in synchrony with the decadal solar cycle, is observed. Sloan and Wolfendale's figure 1 suggests that the decadal cycle in cloud cover has amplitude of about 2%, and it is in synchrony with the decadal solar cycle. Moreover, the same figure shows a downward multidecadal trend in cloud cover of about 4% from 1980 to 2000 that could well agree with the 60-year modulation of the auroras and in the global temperature observed above in Figure 2. The percentages relative to the decadal and 60-year modulation would approximately correspond to about 0.5% and 1% change of the Earth's albedo respectively because these clouds may cover about 30-40% of the Earth. Indeed, Wild (2009) showed that a global solar brightening occurred from 1910 to 1940 and from 1970 to 2000, and global solar dimming occurred from 1940 to 1970: see his figure 9. This 60-year reversal from solar brightening to dimming and from solar dimming to brightening was likely due to a cloud cover 60-year modulation and would support the theory herein presented.

An about 0.5% and 1% albedo change would greatly amplify the climate sensitivity to total solar irradiance, as shown in the above exercise and could also be quantitatively compatible with a 0.1 ^oC climate signature associated to the decadal astronomical cycle (Scafetta, 2009) and with a 0.3/0.4 ^oC natural warming observed from 1970 to 2000, as deduced from the 60-year cyclical modulation of the temperature depicted in Figure 2. These results would be compatible with the empirical climate sensitivity estimated by Scafetta (2009). Thus, the observations appear to be consistent with the theory of an oscillating albedo.

Figure 9 summarizes a chain of mechanisms that, according to the finding of this paper, reasonably links the planetary motion to climate change through solar and heliosphere modulation of the magnetosphere and ionosphere that regulate the cloud cover percentage. The figure updates a figure from Tinsley (2008) where more details about the single physical mechanisms are found. The planets, in particular Jupiter and Saturn, may modulate solar activity, the heliosphere and the magnetosphere in proximity of the Earth. Therefore, a cyclical modulation of the electric properties of the ionosphere occurs, as revealed by the aurora record. This modulation causes a synchronized change of the cloud system through the atmospheric electric circuit. The modulation of the cloud system, together with the solar variations, drives all other climate subsystems including the ocean. All subsystems of the climate synchronize (Scafetta, 2010b; Strogatz, 2009). The resulting output is a global climate system that oscillates with the planetary frequencies. An additional modulation with a period of about 9.1 years is caused by the solar/lunar tidal forces that would act more directly in the ocean and in minor degree on the magnetosphere and ionosphere.

In addition, the variation of the length of the day (LOD) of the Earth has been proposed as another mechanism linking planetary motion to climate change. LOD presents a 60-year cycle (Stephenson and Morrison, 1995; Klyashtorin, 2001; Roberts et al., 2007; Mazzarella, 2008; Mazzarella and Scafetta, 2011; Mörner, 2010; Scafetta, 2010b). Because the LOD 60-year modulation is negatively correlated to the 60-year climate cycle the following mechanism may be working. When the low cloud cover decreases there is an increase of the energy stored in the oceans that causes variations in atmospheric zonal wind circulation and eventually causes more water to move from the equator to the poles, causing a global warming. This toward-pole mass movement induces a LOD decrease because the Earth, by becoming a little bit more spherical, speeds up because of the decrease of its rotational inertia. The latitudinal distribution and transport of energy and momentum associated to changes of zonal winds induced by cloud cover solar-induced changes have been recently advocated also for explaining the presence of a significant solar signature in the semiannual LOD variation (Le Mouël et al., 2010).

8. Reconstruction and forecast of the climate oscillations based on aurora cycles

According Eq. 4, if we can assume that solar irradiance and/or the albedo periodically oscillate, then the temperature at the surface would also oscillate with a similar set of frequencies. In fact, in first approximation, the surface temperature variation would be proportional to the incoming irradiance ΔF.

However, the same result would be obtained also if the heat capacity of the Earth is taken into account. For example, a simple energy balance model could be given by a first order differential equation of the type:

$$\frac{d\Delta T(t)}{dt} = \frac{k\Delta F(t) - \Delta T(t)}{\tau}, \tag{9}$$

where k is a climate sensitivity to the forcing and τ is the thermal relaxation time of the system (Scafetta, 2009). As well known, if the forcing is of the type $\Delta F(t) = \cos(\omega t)$, the solution of the above equation is

$$\Delta T(t) = k\frac{\cos(\omega t) + \omega\tau \sin(\omega t)}{1 + \omega^2\tau^2} + c = A\cos(\omega t + \phi) + c \tag{10}$$

where ϕ and A are given phase and amplitude that depend on ω and τ, and c is a given constant. Indeed, this result emerges from quite general mathematical properties under the approximation of small forced oscillations, and would be also obtained with professional climate GCMs. Thus, if the solar irradiance and/or the albedo are oscillating with a given set of frequencies, then the surface temperature too would present a harmonic component made of the same set of frequencies (in general there may be also sub- and super-harmonics). We would have:

$$\Delta T(t) = A_0 + \sum A_i \cos(\omega_i t + \phi_i). \tag{11}$$

Therefore, as already noted by Lord Kelvin to solve the tidal problem (Thomson, 1881), if the purpose is only to determine the response of the climate system to a harmonic forcing, general mathematical theorems allow us to bypass the problem of accurately solving the single physical mechanisms. Indeed, the parameters A_i and ϕ_i, which would contain all physical information about the climate system, could be easily measured and determined by simple regression on the actual temperature observations.

It is necessary to test whether a harmonic model based on aurora cycles can efficiently both reconstruct and forecast the climate oscillations. In fact, a regression model that uses a set of parameters would be able to fit only the region used to calibrate the model, but if the model is not made of the right dynamical components it will fail any forecasting.

We proceed by assuming, in first approximation, that the global surface temperature record has a harmonic component characterized by a basic set of five periodic signals with periods equal to 9.1, 10.5, 20, 30 and 60 years, as found in the aurora records and in the planetary motion (Scafetta, 2010b). Because the temperature rose from 1850 to 2010, this upward secular trend needs to be detrended from the data because the proposed harmonic model is limited to decadal and multidecadal cycles. We use two fit functions of the type:

$$F_1(t) = A_1(t - 1850)^2 + B_1 \tag{12}$$

and

$$F_2(t) = A_2(t - 1850)^2 + B_2 \; . \tag{13}$$

We use $F_1(t)$ to fit the temperature record from 1850 to 2010. We use $F_2(t)$ to fit the temperature record from 1850 to 1950. We find that $A_1 = 2.9 \cdot 10^{-5} \pm 2 \cdot 10^{-6}\ ^oC/y^2$, $B_1 = -0.41 \pm 0.02\ ^oC$, and that $A_2 = 2.7 \cdot 10^{-5} \pm 2 \cdot 10^{-6}\ ^oC/y^2$, $B_2 = -0.40 \pm 0.02\ ^oC$. We observe that the two acceleration coefficients a_1 and a_2 do not drastically change. This fact may indicate that in 1950 a quadratic fit of the temperature from 1850 to 1950 would have well forecasted the observed 1950-2010 temperature upward trend, but this result is likely a coincidence.

Indeed, the secular upward warming trend may be due to a combination of a millenarian cycle, of a bi-secular cycle, of poorly corrected urban heat island effects (McKitrick and Michaels, 2007; McKitrick, 2010) and of anthropogenic GHG emissions. Scafetta (2009, 2010a) and Loehle and Scafetta (2011) showed that at least 50% of the upward secular trend of the temperature since 1900 could be induced by the correspondent secular increase of the solar activity during this same period. Here we do not investigate further this issue because the above quadratic polynomial fit is not part of the astronomical model, but only a convenient way to represent the trending of the temperature from 1850 to 2010, not outside this period.

That the harmonic model may likely work is already implicit in Figure 10. Here, it is observed a very good synchrony between the quasi 20 and 60-year oscillations of the solar system, which are mostly driven by Jupiter and Saturn, and the correspondent oscillations observed in the climate system.

The astronomical harmonic model must be tested on its forecasting capabilities to be credible. We consider two independent time intervals (1850-1950 and 1950-2010):

$$\begin{aligned} P_1(t) \;=\; & a_1 \cos\left(\frac{2\pi(t-T_1)}{60}\right) + b_1 \cos\left(\frac{2\pi t}{30} + \alpha_1\right) + \\ & c_1 \cos\left(\frac{2\pi(t-T_1)}{20}\right) + d_1 \cos\left(\frac{2\pi t}{10.5} + \beta_1\right) + \\ & e_1 \cos\left(\frac{2\pi t}{9.1} + \gamma_1\right) + f_1 \end{aligned}$$

and

$$\begin{aligned} P_2(t) \;=\; & a_2 \cos\left(\frac{2\pi(t-T_2)}{60}\right) + b_2 \cos\left(\frac{2\pi t}{30} + \alpha_2\right) + \\ & c_2 \cos\left(\frac{2\pi(t-T_2)}{20}\right) + d_2 \cos\left(\frac{2\pi t}{10.5} + \beta_2\right) + \\ & e_2 \cos\left(\frac{2\pi t}{9.1} + \gamma_2\right) + f_2 \end{aligned}$$

In our simplified model, we use $T_1 = 2000.5$ and $T_2 = 1941$, which correspond to the dates of the last two J/S conjunctions of Group I, see Table 2. This choice is also supported by the finding depicted in Figure 10.

We proceed by analyzing three periods. We use the function $F_1(t) + P_1(t)$ to fit the temperature data during two periods: from 1850 to 2010 and from 1950 to 2010. We use the function $F_2(t) + P_2(t)$ to fit the temperature data from 1850 to 1950.

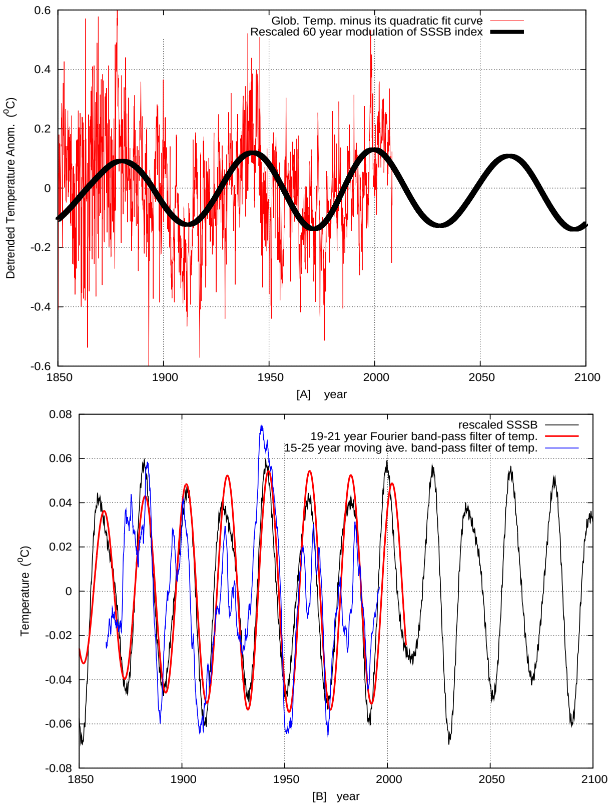

Figure 10: [A] Rescaled 60-year modulation of the solar speed relative to the solar system barycenter (SSSB) (black)[1] (see Figure 6B) against the global surface temperature record detrended of its quadratic fit. [B] Rescaled modulation of the solar speed relative to the solar system barycenter (black) (see Figure 6B) against two alternative pass-band filtered records of the temperature around its two decadal oscillations. The figures clearly indicate a strong coherence between the astronomical oscillations and the oscillations observed in the climate system.

The coefficients of the three regression models are reported in Table 3. We find that the three sets of regression coefficients coincide within the error of measure: both the amplitudes and the phases coincide. The reduced χ_o^2 is 0.34 with 9 degrees of freedom and the coherence probability between the two models is $P_9(\chi^2 \geq \chi_o^2) > 95\%$. Thus, within the limits of the data herein used, it is found that the astronomical harmonic model can both reconstruct and forecast the temperature signal within a high statistical confidence level.

Figure 11A depicts the three regression model outputs against the global surface temperature, which has been smoothed with a four-year moving average algorithm. Figure 11B depicts only the oscillating functions $P_1(t)$, which fits the periods 1850-2010 (solid) and 1950-2010 (dash), and the function $P_2(t)$, which fits the period 1850-1950 (dots). Figure 11A and 11B clearly show a very good matching during the entire period 1850-2010 between the decadal and multidecadal climate oscillations and the oscillations reconstructed by the models in all three cases.

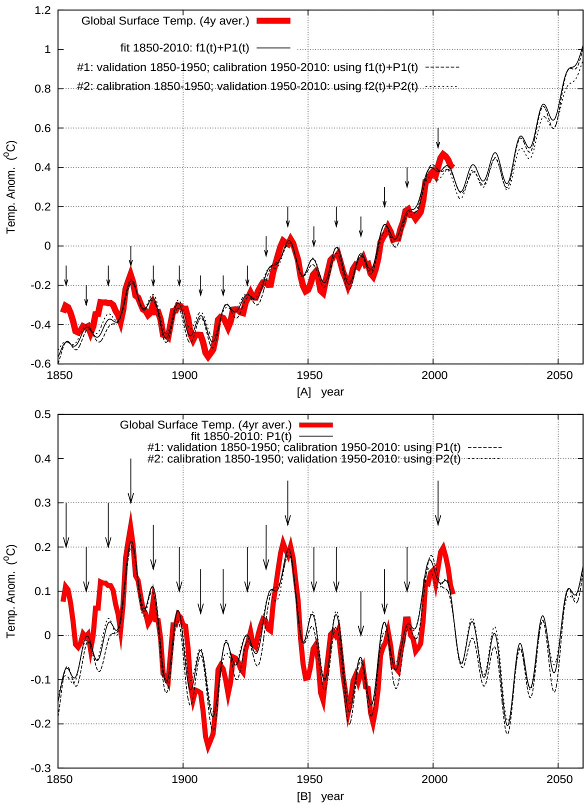

Figure 11: Astronomical harmonic constituent model reconstruction and forecast of the global surface temperature.[1] [A] Four year moving average of the global surface temperature against the climate reconstructions obtained by using the function $F_1(t) + P_1(t)$ to fit the period 1850-2010 (black solid) and the period 1950-2010 (dash), and the function $F_2(t) + P_2(t)$ to fit the period 1850-1950 (dots). [B] The functions $P_1(t)$ and $P_2(t)$ represent the periodic modulation of the temperature reproduced by the celestial model based on the five aurora major decadal and multidecadal frequencies. The arrows indicate the local decadal maxima where the good matching between the data patterns and the models is observed. Note that in both figures the three model curves almost coincide for more than 200 years and well reconstruct and forecast the temperature oscillations.

The result depicted in the figure implies that if we were in 1950, by using an astronomical harmonic constituent model based on aurora cycles and on the temperature record from 1850 to 1950, it could have been possible to forecast with a reasonable accuracy the climate oscillations within a decadal and multidecadal scale occurring from 1950 to 2010. The figure also implies the opposite, that is, that the decadal and multidecadal climate oscillations from 1850 to 1950 could be forecasted by using the same astronomical harmonic constituent model calibrated on the temperature data from 1950 to 2010. Note that during the period 1915-1940 the decadal cycle appear to disappear because during this period the 9.1 and 10.5 year cycles interfere destructively. The remarkable result depicted in Figure 11 does imply that the climate oscillations within the secular scale can be accurately forecasted by using the major decadal frequencies found in the mid-latitude aurora records, which appear to be driven by astronomical cycles associated to the movement of Jupiter and Saturn (about 10, 20, 30 and 60 years), to the lunar cycle (9.1 years) and to the 11-year solar cycle.

About the imminent future, Figure 11A suggests that if the quadratic background upward trend of the temperature continues during the next decades, the global temperature may remain approximately constant until 2030-2040, and this result would be approximately compatible with that found in Loehle and Scafetta (2011) by using a different methodology that yield a net anthropogenic warming component of about $+0.66\ ^{o}C/century$ from 1940 to 2050 against the IPCC estimate of $+2.3\ ^{o}C/century$ during the same period. However, the quadratic trend used here should not be trusted after 2040 also because is not part of the harmonic model, but only a convenient way to fit the temperature from 1850 to 2010.

The observed warming since 1850 could have been partially caused by a large quasi-millennial climate cycle, which has caused the Medieval Warm Period, the Little Ice Age and the Modern Warm Period. Probably this large quasi-millennial cycle just entered or is going to enter into its cooling phase and, therefore, it can further cool the planet on a multi-secular scale. Other cooling natural component can derive from a bi-secular natural solar induced cycle. These cycles are known to have regulated multidecadal cold periods (the well-known Oort, Wolf, Spörer, Maunder, Dalton minima). In fact, as noted in Scafetta (2010a) the last four sunspot cycles (#20-21-22-23) look quite similar to the four sunspot cycles (#1-2-3-4) that occurred just before the Dalton minimum. That the Sun may be entering in a prolonged period of minimum activity is reasonable (Duhau and de Jager, 2010). That a multi-secular climate natural cycle may be turning down is also indirectly suggested by the fact that since 1930 the sea-level acceleration has been, on average, slightly negative (Houston and Dean, 2011). Interestingly, the measured deceleration of the sea-level rise from 1930 to 2010 occurred despite the strong positive acceleration of anthropogenic GHG emissions during the same period, which would indicate that other more powerful forcings (such as an astronomical forcing of the cloud system) are the major regulators of climate change.

9. Conclusion

Four centuries ago, Johannes Kepler explained that earthly nature couldn't help but respond to the dictates of heavenly harmonies, and said that nature is affected by an aspect *just as a farmer is moved by music to dance* (Kemp, 2009). Kepler clearly shared the common belief of his time that the climate was influenced by astronomical cycles and understood the subtle phenomenon of *collective synchronization* that has been extensively studied in nonlinear complex science since the times of Huygens (Pikovsky et al., 2001; Strogatz, 2009; Scafetta, 2010b). Indeed, climate change records present geometrical characteristics that suggest that climate is synchronized, probably through the Sun and the heliosphere, to complex astronomical cycles driven by planetary harmonics.

In this paper, we have studied the historical record of mid-latitude auroras from 1700 to 1900, and of the Faroes Islands from 1873 to 1966 to search for a possible physical mechanism linking planetary motion to climate. We have shown that mid-latitude aurora records and the global surface temperature record share a set of oscillations with periods of about 9.1, 10-11, 20-21, 30 and 60-62 years. Other shorter and longer oscillations may be present, but they are not discussed here. In particular, clear quasi 60-year cycles in the aurora records are synchronized to the 60-year cycle observed in the global surface temperature and in multi-secular proxy climate reconstructions of both the Atlantic and Pacific climatic oscillations since 1650 and in Indian summer monsoon records. Charvátová-Jakubcová et al. (1988) found that a large 60-year cycle is present in the mid-latitude aurora record also for the longer period from 1001 to 1900 and other planetary frequencies are present as well in the millennial aurora record. Numerous other studies have found quasi 10, 20 and 60-year cycles in multiple climate records and in astronomical records, as summarized in the Introduction. By taking into account the results of Scafetta (2010b), this synchrony exists also with the global ocean and land global surface temperature records of both hemispheres.

The aurora record cycles reveal a direct or indirect planetary influence on the Sun and on the Earths magnetosphere and ionosphere. Indeed, proxy reconstructions may suggest a 60-year cycle in the total solar irradiance (TSI) was almost stable or slightly decreased from 1880 to 1910, and it increased from 1910 to 1940. From 1940 to 1970 TSI may have decreased as the TSI reconstruction of Hoyt and Schatten (1997) suggests. Hoyt and Schatten's TSI reconstruction well correlates with the temperature records during the last century (Soon, 2009). Finally, an increase of the solar activity from 1970 to 2000 and a decrease afterward would be supported by the ACRIM TSI satellite composite, which may more faithfully reproduce the satellite observations Willson and Mordvinov (2003); Scafetta and Willson (2009); Scafetta (2011) (but not by the PMOD composite Fröhlich and Lean (1998), which is the TSI record preferred by the IPCC (2007)). Thus, solar activity could have been characterized by a quasi 60-year modulation superimposed to other larger secular, bi-secular and millennial cycles (Křivský, 1984; Ogurtsov et al., 2002), although it may not appear evident in every total solar irradiance reconstruction (Krivova et al., 2007; Wang et al., 2005).

It is possible that when Jupiter and Saturn are closer to the Sun, there may be an increased solar activity because of the stronger planetary tides and other mechanisms (Wolff and Patrone, 2010), and a stronger magnetic field within the inner region of the solar system form, although the patterns may be more complicated because of the presence of other cycles that will be discussed in another paper. A stronger solar or heliospheric magnetic field better screens galactic cosmic ray fluxes. Fewer cosmic rays reaching the Earth imply a weaker ionization of the upper atmosphere. As a side-effect, less auroras form in the middle latitudes because a stronger magnetic field and a less ionized ionosphere mostly constrains the auroras in the polar region. In addition, the level of ionization of the atmosphere has been proposed as an important mechanism that can modulate the low cloud cover formation (Tinsley, 2008;

Kirkby, 2007; Svensmark et al., 2009). Essentially, when the ionization is weaker, less clouds form. A solar and heliospheric modulation of the cloud system would greatly contribute to climate change through an albedo modulation (see Eq. 8). The above sequence of mechanisms would explain why the climate presents oscillations at multiple frequencies that are synchronized with the aurora and the planetary cycles.

We have used a phenomenological harmonic model based on five decadal and multidecadal frequencies with periods of 9.1, 10.5, 20, 30 and 60 years that has been detected in the aurora records and that could be associated to evident astronomical and solar/lunar tidal cycles. We have shown that it is possible to forecast the climate oscillations occurred from 1950 to 2010 using the climatic information derived from the period 1850-1950 and the frequency information deduced from the mid-latitude aurora before 1900. Analogously, we have shown that it is possible to forecast the climate oscillations that occurred backward from 1850 to 1950 using the information derived from the period 1950-2010. Thus, these findings strongly support the thesis that the climate oscillations can be approximately forecasted by using astronomical cycles. The proposed astronomical harmonic constituent model for climate change based on aurora cycles is conceptually equivalent to the commonly used tide-predicting machines based on planetary harmonic constituent analysis conceived by Lord Kelvin in 1867.

Interestingly, the traditional Chinese, Tamil and Tibetan calendars are arranged in major 60-year cycles (Aslaksen, 1999). Perhaps, these sexagenarian cyclical calendars were inspired by climatic and astronomical observations and were used for timing and regulating human business. For example, even ancient Sanskrit texts report about a 60-year monsoon rainfall cycle (Iyengar, 2009) and associate it to the movement of Jupiter and Saturn, the *Brihaspati* 60-year cycle, which may explain why Asian populations used sexagesimal calendars. Indeed, a 60-year cycle linked to Jupiter and Saturn was extremely well known to several ancient civilizations (Temple, 1998). The major cycles discussed in this paper are also approximately found in the major business cycles (Pustilnik and Din, 2004; Korotayev and Tsirel, 2010). A link between planetary motion, climate and economy (which mostly in the past could be driven by agricultural productivity) would ultimately explain the interest of the ancient civilizations in tracking the position of the planets and their attempts in developing multiscale cyclical calendars (Ptolemy, 2nd century; Maʻšar, 886; Swerdlow, 1998).

In conclusion, the results presented here strongly support and reinforce the argument of Scafetta (2010a,b) that the climate is forced by astronomical oscillations related to the Sun, the Moon and the planets, and, as Figure 11 shows, a significant component of it can be forecasted within an acceptable uncertainty with appropriate harmonic models.

References

Adhikari, D. P., and F. Kumon, 2001. Climatic changes during the past 1300 years as deduced from the sediments of Lake Nakatsuna, central Japan. Limnology 2, 157-168.

Agnihotri, R., K. Dutta, R. Bhushan, and B. L. K. Somayajulu, 2002. Evidence for solar forcing on the Indian monsoon during the last millennium. Earth and Planetary Science Letters, 198, 521527.

Agnihotri, R., and K. Dutta, 2003. Centennial scale variations in monsoonal rainfall (Indian, east equatorial and Chinese monsoons): Manifestations of solar variability. Current Science 85, 459-463. India summer monsoon data from IRI Climate Data Library; http://ingrid.ldeo.columbia.edu/SOURCES/Indices/india/rainfall

Aslaksen, H., (1999). The mathematics of the Chinese calendar, *National University of Singapore.* http://www.math.nus.edu.sg/aslaksen/calendar/chinese.shtml

Bard, E., G. Raisbeck, F. Yiou, and J. Jouzel, 2000. Solar irradiance during the last 1200 years based on cosmogenic nuclides. Tellus 52B, 985-992.

Bendandi, R., 1931. Un Principio Fondamentale dell'Universo. (S.T.E., Faenza, Italy).

Bennett, J., M. Donahue, N. Schneider and M. Voit, 2010. *The cosmic Perspective* (sixth edition), Pearson Addison-Wesley, San Francisco.

Black, D. E., L. C. Peterson, J. T. Overpeck, A. Kaplan, M. N. Evans, and M. Kashgarian, 1999. Eight Centuries of North Atlantic Ocean Atmosphere Variability. Science 286, 1709-1713.

Bond, G., B. Kromer, J. Beer, R. Muscheler, M. N. Evans, W. Showers, S. Hoffman, R. Lotti-Bond, I. Hajdas, and G. Bonani, 2001. Persistent Solar Influence on North Atlantic Climate During the Holocene. Science 294, 2130-2136.

Brohan, P., J. J. Kennedy, I. Harris, S. F. B. Tett and P. D. Jones, 2006. Uncertainty estimates in regional and global observed temperature changes: a new dataset from 1850. J. Geophys. Res. 111, D12106.

Brown, B. H., 2008. Short-term changes in global cloud cover and in cosmic radiation. J. of Atm. and Solar-Terrestrial Physics 70, 1122-1131.

Bucha, V., I. Jakubcová, and M. Pick, 1985. Resonance frequencies in the Suns motion. Studia Geophysica et Geodetica 29, 107111.

Camuffo, D., 2001. Lunar Influences On Climate. Earth, Moon and Planets 8586, 99-113.

Camuffo, D., et al., 2010. 500 year temperature reconstruction in the Mediterranean Basin by means of documentary data and instrumental observations. Clim. Change 101, 169-199.

Charvátová-Jakubcová, I., J. Střeštík, and L. Křivský, 1988. The periodicity of aurorae in the years 1001-1900. Stud. Geophys. Geod. 32, 70-77.

Charvátová, I., 1990. The relation between solar motion and solar variability. Bull. Astron. Inst. Czechosl. 41, 56-59.

Charvátová, I., 2000. Can origin of the 2400-year cycle of solar activity be caused by solar inertial motion? Ann. Geophysicae 18, 399-405.

Charvátová, I., and J. Střeštík, 2004. Periodicities between 6 and 16 years in surface air temperature in possible relation to solar inertial motion. J. of Atm. and Solar-Terr. Phys. 66, 219-227.

Charvátová, I., 2009. Long-term predictive assessments of solar and geomagnetic activities made on the basis of the close similarity between the solar inertial motions in the intervals 1840-1905 and 1980-2045. New Astronomy 14, 25-30.

Courtillot, V., J. L. Le Mouël, and P. N. Mayaud (1977). Maximum Entropy Spectral Analysis of the Geomagnetic Activity Index aa Over a 107-Year Interval, J. Geophys. Res., 82(19), 2641-2649.

Courtillot, V., and Renne, P., 2003. On the ages of flood basalt events, C. R. Geoscience 335, 113-140.

Cook, T. L., R. S. Bradley, J. S. Stoner and P. Francus, 2009. Five thousand years of sediment transfer in a high arctic watershed recorded in annually laminated sediments from Lower Murray Lake, Ellesmere Island, Nunavut, Canada. J. of Paleolimnology 41, 77-94.

Currie, R. G., 1984. Evidence for 18.6 year lunar nodal drought in western North America during the past millennium. J. Geophys. Res. 89, 1295-1308.

Doodson, A. T., 1921. The harmonic development of the tide-generating potential. Proceedings of the Royal Society of London, Series A 100 (704), 305-329.

Douglass, D. H., and B. D. Clader, 2002. Climate sensitivity of the Earth to solar irradiance. Geophys. Res. Lett., 29, doi: 10.1029/2002GL015345.

Duhau, S., and C. de Jager, (2010). The Forthcoming Grand Minimum of Solar Activity. J. of Cosmology 8, 1983-1999.

Eddy, J. A., 1976. The Maunder Minimum. Science 192, 1189-1202.

Ehret, T., 2008. Old Brass Brains - Mechanical Prediction of Tides. ACSM Bulletin, 41-44.

Eichler A., S. Olivier, K. Henderson, A. Laube, J. Beer, T. Papina, H. W. Gäggeler, M. Schwikowski, 2009. Temperature response in the Altai region lags solar forcing. Geophys. Res. Lett. 36, L01808, doi:10.1029/2008GL035930.

Fairbridge, R. W., and J. H. Shirley, 1987. Prolonged minima and the 179-yr cycle of the solar inertial motion. Solar Phys. 110, 191-210.

Feynman, J., and P. F. Fougere, 1984. Eighty-year periodicity in solar-terrestrial penomena confirmed. J. Geophys Res. 89, 3023-3027.

Fischer, E. G., 1912. The Coast and Geodetic Survey Tide Predicting Machine No. 2. Popular Astronomy 20, 269-285.

Fröhlich, C., and J. Lean, 1998. The Sun's total irradiance: cycles, trends and related climate change uncertainties since 1978. Geophys. Res. Lett. 25, 4377-4380.

Ge, Q.-S., J. Y. Zheng, Z.-X. Hao, X.-M. Shao, W.-C. Wang, and J. Luterbacher, 2010. Temperature variation through 2000 years in China: An uncertainty analysis of reconstruction and regional difference. Geophysical Research Letters, 37, L03703.

Ghil M., R. M. Allen, M. D. Dettinger, K. Ide, D. Kondrashov, M. E. Mann, A. Robertson, A. Saunders, Y. Tian, F. Varadi, and P. Yiou, 2002. Advanced spectral methods for climatic time series. Rev. Geophys. 40, 3.1-3.41. SSA-MTM tool kit for spectral analysis.

Goswami, B. N., M. S. Madhusoodanan, C. P. Neema, and D. Sengupta, 2006. A physical mechanism for North Atlantic SST influence on the Indian summer monsoon. Geophys. Res. Lett. 33, L02706.

Grandpierre, A., 1996. On the origin of the solar cycle periodicity. Astrophysics and Space Science 243, 393-400.

von Gunten L., M. Grosjean, B. Rein, R. Urrutia and P. Appleby, 2009. A quantitative high-resolution summer temperature reconstruction based on sedimentary pigments from Laguna Aculeo, central Chile, back to AD 850. The Holocene 19, 873-881.

Harrison, G., and D. Stephenson, 2005. Empirical evidence for a nonlinear effect of galactic cosmic rays on clouds. Pro. of Roy. Soc. A 462, 1-13.

Hayden, H. C., 2007. A primer on CO_2 and climate, (Vales Lake Publishing, LLC).

Hood, L. L., and J. L., Jirikowic, 1991. A probable 2400 year solar quasi-cycle in atmospheric delta ^{14}C. Holocene 12, 98-105.

Houston, J. R. and Dean R. G., 2011. Sea-Level Acceleration Based on U.S. Tide Gauges and Extensions of Previous Global-Gauge Analyses. J. of Coastal Research. DOI: 10.2112/JCOASTRES-D-10-00157.1

Hoyt, D. V., and K. H. Schatten, 1997. The Role of the Sun in the Climate Change. (Oxford Univ. Press, New York).

Huang, S. P., H. N. Pollack, and P.-Y. Shen, 2008. A late Quaternary climate reconstruction based on borehole heat flux data, borehole temperature data, and the instrumental record. Geophys. Res. Lett. 35, L13703.

Hung, C-C., 2007. Apparent Relations Between Solar Activity and Solar Tides Caused by the Planets. Report NASA/TM-2007-214817. http://gltrs.grc.nasa.gov/Citations.aspx?id=330

Idso, C., and S. F. Singer, 2009. Climate Change Reconsidered: 2009 Report of the Nongovernmental Panel on Climate Change (NIPCC) Chicago, IL: The Heartland Institute.

IPCC: Solomon, S. et al. (eds) in Climate Change 2007: The Physical Science Basis.Contribution of Working Group I to the Fourth Assessment Report of the Intergovernmental Panel on Climate Change, (Cambridge University Press, Cambridge, 2007).

Iyengar, R. N., 2009. Monsoon rainfall cycles as depicted in ancient Sanskrit texts. Current science 97, 444-447.

Jevrejeva, S., J. C. Moore, A. Grinsted, and P. L. Woodworth, 2008. Recent global sea level acceleration started over 200 years ago? Geophys. Res. Lett. 35, L08715.

Jose, P. D., 1965. Suns motion and Sunspots, Astronomical Journal 70, 193-200.

Keeling, C. D., and T. P. Whorf, 2000. The 1,800-year oceanic tidal cycle: A possible cause of rapid climate change. PNAS 97-8, 3914-3819.

Keigwin, L. D., 1996. The Little Ice Age and Medieval Warm Period in the Sargasso Sea. Science 274, 1503-1508.

Kellerhals, T., S. Brütsch, M. Sigl, S. Knüsel, H. W. Gäggeler, and M. Schwikowski, 2010. Ammonium concentration in ice cores: A new proxy for regional temperature reconstruction? J. Geophys. Res. 115, D16123.

Kemp, M., 2009. Johannes Kepler on Christmas. Nature 462, 24.

Kepler, J., 1606. De Stella Nova in Pede Serpentarii, (Pragae, Typis Pauli Sessii).

Kerr, R. A., 2001. A Variable Sun Paces Millennial Climate. Science 294, 1431-1433.

Khim, B.-K., H. I. Yoon, C. Y. Kang and J. J. Bahk, 2002. Unstable climate oscillations during the Late Holocene in the Eastern Bransfield Basin, Antarctic Peninsula. Quaternary Research 58, 234-245.

Kirkby J., 2007. Cosmic Rays and Climate. Surveys in Geophys. 28, 333-375.

Klyashtorin, L. B., 2001. Climate change and long-term fluctuations of commercial catches: the possibility of forecasting. FAO Fisheries Technical Paper No. 410 Rome, FAO.

Klyashtorin, L. B. and A. A. Lyubushin, 2007. Cyclic Climate Changes and Fish Productivity. Moscow, VNIRO Publishing.

Klyashtorin, L. B., V. Borisov, and A. Lyubushin, 2009. Cyclic changes of climate and major commercial stocks of the Barents Sea. Mar. Biol. Res. 5, 4-17.

Knutti, R., and G. C. Hegerl, 2008. The equilibrium sensitivity of the Earth temperature to radiation changes. Nature Geoscience 1, 735-743.

Komitov, B., 2009. The Sun-climate relationship II: The cosmogenic beryllium and the middle latitude aurora. Bulgarian Astronomical Journal 12, 75-90.

Korotayev A. V., and S. V. Tsirel, 2010. A Spectral Analysis of World GDP Dynamics: Kondratieff Waves, Kuznets Swings, Juglar and Kitchin Cycles in Global Economic Development, and the 2008-2009 Economic Crisis. Structure and Dynamics 4, 3-57.

Krivova N. A., Balmaceda L., Solanki S. K., 2007. Reconstruction of solar total irradiance since 1700 from the surface magnetic flux. Astronomy and Astrophysics 467, 335-346.

Křivský, L. 1984. Long-term fluctuations of solar activity during the last thousand years. Solar Physics 93, 189-194.

Křivský L. and K. Pejml, 1988. Solar activity, aurorae and climate in Central Europe in the last 1000 years. Bul. Astron. Inst. Chechosl. Acad. Sci. No75. http://www.ngdc.noaa.gov/stp/aeronomy/aurorae.html

Knudsen, M. F., Seidenkrantz M-S., Jacobsen B. H. and Kuijpers A., 2011. Tracking the Atlantic Multidecadal Oscillation through the last 8,000 years. Nature Communications 2, #178.

Lamb H. H., 1965. The early medieval warm epoch and its sequel. Palaeogeography, Palaeoclimatology, Palaeoecology 1, 13-37.

Laken B. A., D. R. Kniveton, and M. R. Frogley, 2010. Cosmic rays linked to rapid mid-latitude cloud changes. Atmos. Chem. Phys. 10, 10941-10948.

Landscheidt, T., 1988. Solar rotation, impulses of the torque in Sun's motion, and climate change. Climatic Change 12, 265-295.

Landscheidt, T., 1999. Extrema in Sunspot cycle linked to Sun's motion. Solar Physics 189, 415-426.

Lauer, A., K. Hamilton, Y. Wang, V. T. Phillips, and R. Bennartz, 2010. The Impact of Global Warming on Marine Boundary Layer Clouds over the Eastern Pacific A Regional Model Study. Journal of Climate 23(21), 5844-5863.

Lean, J. L., Rind, D. H., 2008. How natural and anthropogenic influences alter global and regional surface temperatures: 1889 to 2006. Geophys. Res. Lett. 35, L18701.

Lindzen, R. S., and Y-S. Choi, 2011. On the Observational Determination of Climate Sensitivity and Its Implications, Asia-Pacific J. Atmos. Sci., 47(4), 377-390.

Ljungqvist, F. C., 2009. Temperature proxy records covering the last two millennia: a tabular and visual overview. Geogr. Ann. 91A, 11-29.

Ljungqvist, F. C., 2010. A new reconstruction of temperature variability in the extra-tropical Northern Hemisphere during the last two millennia. Geografiska Annaler: Physical Geography, 92, 339-351.

Loehle, C., and J. H. Mc Culloch, 2008. Correction to: A 2000-year global temperature reconstruction based on non-tree ring proxies. Energy Environ. 19, 93-100.

Loehle, C., and N. Scafetta, 2011. Climate Change Attribution Using Empirical Decomposition of Climatic Data. The Open Atmospheric Science Journal, 5, 74-86.

van Loon, H., and K. Labitzke, 2000. The influence of the 11-year solar cycle on the stratosphere below 30km: A review. Space Sci. Rev. 94, 259-278.

Mackey R., 2007. Rhodes Fairbridge and the idea that the solar system regulates the Earth's climate. J. of Coastal Res. 50, 955-968.

de Mairan J. J. D., 1733. Traite Physique et Historique de l'Aurore Boreale, Imprimerie Royale, Paris.

MacDonald, G. M., and R. A. Case, 2005. Variations in the Pacific Decadal

Oscillation over the past millennium. Geophys. Res. Lett. 32, L08703.

McKinnell, S. M., and W. R. Crawford, 2007. The 18.6-year lunar nodal cycle and surface temperature variability in the northeast Pacific. J. Geophys. Res. 112, C02002.

Mann, M. E., and P. D. Jones, 2003. Global surface temperature over the past two millennia. Geophy. Res. Lett. 30, 1820-1824.

Mann, M. E., Z. Zhang, M. K. Hughes, R. S. Bradley, S. K. Miller, S. Rutherford, and F. Ni, 2008. Proxy-based reconstructions of hemispheric and global surface temperature variations over the past two millennia. PNAS 105, 13252-13257.

Ma‘šar A., 886. On the great conjunctions. Edited and translated by K. Yamamoto and C. Burnett, (Brill, 2000).

Mazzarella, A., 2008. Solar Forcing of Changes in Atmospheric Circulation, Earth’s Rotation and Climate. The Open Atmospheric Science Journal 2, 181-184.

Mazzarella, A. and N. Scafetta, 2011. Evidences for a quasi 60-year North Atlantic Oscillation since 1700 and its meaning for global climate change, Theor. Appl. Climatol. DOI 10.1007/s00704-011-0499-4

McKitrick, R. and P. Michaels, 2007. Quantifying the influence of anthropogenic surface processes and inhomogeneities on gridded global climate data. J. of Geophysical Research 112, D24S09.

McKitrick, R., 2010. Atmospheric circulations do not explain the temperature-industrialization correlation. Statistics, Politics, and Policy 1, 1. DOI: 10.2202/2151-7509.1004

McShane, B. B., and A. J. Wyner, 2011. A Statistical Analysis of Multiple Temperature Proxies: Are Reconstructions of Surface Temperatures Over the Last 1000 Years Reliable? The Annals of Applied Statistics 5(1), 5-44.

Meehl, G. A., J. M. Arblaster, K. Matthes, F. Sassi, and H. van Loon, 2009. Amplifying the Pacific Climate System Response to a Small 11-Year Solar Cycle Forcing. Science 325, 1114-1118.

Milankovic, M., 1941. Canon of insolation and the ice-age problem, (Kanon der Erdbestrahlung und seine Anwendung auf das Eiszeitenproblem) , Belgrade, 1941 (Royal Serbian Academy of Mathematical and Natural Sciences, v. 33).

Moberg A., D. M. Sonechkin, K. Holmgren, N. M. Datsenko, and W. Karlén, 2005. Highly variable Northern Hemisphere temperatures reconstructed from low- and high-resolution proxy data. Nature 433, 613-617.

Mörner, N.-A., 2010. Solar Minima, Earth’s rotation and Little Ice Ages in the past and in the future, Glob. Planet. Change, doi:10.1016/j.gloplacha.2010.01.004

Le Mouël J-L., Courtillot V., E. Blanter, and M. Shnirman, 2008. Evidence for a solar signature in 20th-century temperature data from the USA and Europe. Geoscience 340, 421-430.

Le Mouël, J.L., E. Blanter, M. Shnirman, and V. Courtillot, 2010. Solar forcing of the semi]annual variation of lengthofday, Geophys. Res. Lett., 37, L15307.

Munk, W., and B. Bills, 2007. Tides and the climate: Some speculations. J. of Physical Oceanography 37, 135-147.

Ogurtsov, M. G., Y. A. Nagovitsyn, G. E. Kocharov, and H. Jungner, 2002. Long-period cycles of the Suns activity recorded in direct solar data and proxies. Solar Phys. 211, 371-394.

Okal, E., and Anderson, D. L., 1975. Planetary Theory of sunspots. Nature 253, 511-513.

Olmsted, D., 1856. On the Recent Secular Period of the Aurora Borealis. (Smithsonian Contributions to Knowledge, vol. 8).

Oppo D. W., Y. Rosenthal, and B. K. Linsley, 2009. 2,000-year-long temperature and hydrology reconstructions from the Indo-Pacific warm pool. Nature 460, 1113-1116.

Parker D. E., T. P. Legg, and C. K. Folland, 1992. A new daily Central England Temperature Series, 1772-1991. Int. J. Clim. 12, 317-342.

Patterson, R. T., A. Prokoph, and A. Chang, 2004. Late Holocene sedimentary response to solar and cosmic ray activity influenced climate variability in the NE Pacific. Sedimentary Geology 172, 67-84.

Perryman, M. A. C., and Schulze-Hartung T., 2010. The barycentric motion of exoplanet host stars Tests of solar spinorbit coupling. Astronomy & Astrophysics 525, 15668.

Pikovsky, A., M. Rosemblum and J. Kurths, 2001. Synchronization: A Universal Concept in Nonlinear Sciences. (Cambridge University Press).

Priestly, M. B., 2001. Spectral analysis and time series , Academic Press, London eleventh printing.

Ptolemy, C., 2nd century. Tetrabiblos, compiled and edited by F. E. Robbins, Cambridge, MA. Harvard University Press (Loeb Classical Library 1940).

Pustilnik, L. A., and G. Y. Din, 2004. Influence of solar activity on the state of the wheat market in medieval England, Solar Physics 223, 335356.

Raspopov, O. M., V. A. Dergachev, J. Esper, O. V. Kozyreva, D. Frank, M. Ogurtsov, T. Kolström, and X. Shao, 2008. The influence of the de Vries (200-year) solar cycle on climate variations: Results from the Central Asian Mountains and their global link. Palaeogeography, Palaeoclimatology, Palaeoecology 259, 6-16.

Roberts, P. H., Z. J. Yu, and C. T. Russell, 2007. On the 60-year signal from the core. Geophysical & Astrophysical Fluid Dynamics 101, 11-35.

Rockström J., et al., 2009. A safe operating space for humanity, Nature 461, 472-475.

Roe G., 2006. In defense of Milankovitch. Geophysical Research Letters 33, L24703.

Rohs S., R. Spang, F. Rohrer, C. Schiller, and H. Vos, 2010. A correlation study of high-altitude and midaltitude clouds and galactic cosmic rays by MIPAS-Envisat. J. Geophys. Res. 115, D14212.

Scafetta, N., and B. J. West, 2005. Estimated solar contribution to the global surface warming using the ACRIM TSI satellite composite, Geophys. Res. Lett. 32, doi:10.1029/2005GL023849.

Scafetta, N., and B. J. West, 2007. Phenomenological reconstructions of the solar signature in the Northern Hemisphere surface temperature records since 1600. J. Geophys. Res. 112, D24S03.

Scafetta, N. and B. J. West, 2008. Is climate sensitive to solar variability? Physics Today 3, 50-51.

Scafetta, N., and R. C. Willson, 2009. ACRIM-gap and TSI trend issue resolved using a surface magnetic flux TSI proxy model. Geophys. Res. Lett. 36, L05701.

Scafetta, N., 2009. Empirical analysis of the solar contribution to global mean air surface temperature change. J. Atm. and Solar-Terr. Phys. 71, 1916-1923.

Scafetta, N., 2010a. Climate Change and Its causes, A Discussion about Some Key Issues. La Chimica e l’Industria 1, 70-75. English translation published by Science and Public Policy Institute (http://scienceandpublicpolicy.org/originals/climate_change_causes.html).

Scafetta, N., 2010b. Empirical evidence for a celestial origin of the climate oscillations and its implications. Journal of Atmospheric and Solar-Terrestrial Physics 72, 951-970.

Scafetta, N., 2011. Total Solar Irradiance Satellite Composites and their Phenomenological Effect on Climate,” chapter 12, pag 289-316. In “Evidence-Based Climate Science: Data opposing CO2 emissions as the primary source of global warming” edited by Don Easterbrook, Elsevier).

Schulz, M., and A. Paul 2002. Holocene Climate Variability on Centennial-to-Millennial Time Scales: 1. Climate Records from the North-Atlantic Realm, 41-54. in Wefer, G. Berger, W., Behre, K-E., Jansen, E. eds, Climate Development and History of the North Atlantic Realm. (Springer-Verlag Berlin Heidelberg).

Schuster, A., 1911. The Influence of Planets on the Formation of Sun-Spots. Proceedings of the Royal Society of London. Series A, Containing Papers of a Mathematical and Physical Character 85 (579), 309-323.

Shaviv, N. J., 2003. The Spiral Structure of the Milky Way, Cosmic Rays, and Ice Age Epochs on Earth. New Astronomy 8, 39-77.

Shaviv, N. J., and J. Veizer, 2003. Celestial driver of Phanerozoic climate? GSA Today 13, 4-10.

Shaviv, N. J., 2008. Using the oceans as a calorimeter to quantify the solar radiative forcing. J. Geophys. Res. 113, A11101.

Silverman, S. M. 1992. Secular variation of the aurora for the past 500 years. Reviews of Geophysics 30, 333-351.

Sinha, A., K. G. Cannariato, L. D. Stott, H.-C. Li, C.-F. You, H. Cheng, R. L. Edwards, and I. B. Singh, 2005. Variability of Southwest Indian summer monsoon precipitation during the Bølling-Ållerød. Geology 33, 813-816.

Sidorenkov, N. S., and I. Wilson, 2009. The decadal fluctuations in the Earth’s rotation and in the climate characteristics. In: Proceedings of the “Journees 2008 Systemes de reference spatio-temporels” , M. Soffel and N. Capitaine (eds.), Lohrmann-Observatorium and Observatoire de Paris., 174-177.

Siscoe, G. L., 1980. Evidence in the auroral record for secular solar variability. Rev. Geophys. 18, 647-658.

Sloan, T., and A. W. Wolfendale, 2008. Testing the proposed causal link between cosmic rays and cloud cover. Envir. Res. Lett. 3, 024001.

Solomon, S., G.-K. Plattner, R. Knutti and P. Friedlingstein, 2009. Irreversible climate change due to carbon dioxide emissions, PNAS 106, 1704-1709.

Solomon S. et al., 2010. Contributions of stratospheric water vapor to decadal changes in the rate of global warming, Science Express 327, 1219-1223.

Sonett, C. P., and H. E. Suess, 1984. Correlation of bristlecone pine ring widthswith atmospheric carbon-14 variations: a climate-sun relation. Nature 308, 141-143.

Soon, W. W.-H., 2009. Solar Arctic-Mediated Climate Variation on Multi-decadal to Centennial Timescales: Empirical Evidence, Mechanistic Explanation, and Testable Consequences, Physical Geography 30, 144-184.

Spencer, R.W. and Braswell, W.D., 2011. On the Misdiagnosis of Surface Temperature Feedbacks from Variations in Earth’s Radiant Energy Balance. Remote Sens. 3, 1603-1613.

Steinhilbe,r F., Beer J., and Fröhlich C., 2009. Total solar irradiance during the Holocene. Geophys. Res. Lett. 36, L19704.

Stephenson, F. R., and L. V. Morrison, 1995. Long-term fluctuations in Earth’s rotation: 700 BC to AD 1990. Philos. Trans. R. Soc. A 351, 165-202.

Strogatz, S. H., 2009. Exploring complex networks, Nature 410, 268-276.

Stuber, N., M. Ponater, and R. Sausen, 2001. Is the climate sensitivity to ozone perturbations enhanced by stratospheric water vapor feedback? Geophys. Res. Lett. 28, 2887-2890.

Sturrock, P. A., J. D. Scargle, G. Walther and M. S. Wheatland, 2005. Combined and comparative analysis of power spectra. Solar Physics 227, 137-153.

Suess, H.E., 1980. The radiocarbon record in tree rings of the last 8000 years. Radiocarbon 22, 200-209.

Svensmark, H., 1998. Influence of Cosmic Rays on Earth’s Climate. Physical Review Letters 81(22), 5027-5030.

Svensmark, H., 2007. Cosmoclimatology: A New Theory Emerges. Astronomy & Geophysics 48, 1.18-1.24.

Svensmark, H., Bondo T, and Svensmark J., 2009. Cosmic ray decreases affect atmospheric aerosols and clouds, Geophysical Research Letters 36, L15101.

Swerdlow, N. M., 1998. The Babylonian Theory of the Planets (Princeton University Press).

Taylor, J.R., 2005. Classical Mechanics, University Science Books.

Temple, R. K. G., 1998. The Sirius Mystery. Destiny Books. in ‘Appendix III: Why Sixty years?” http://www.bibliotecapleyades.net/universo/siriusmystery/siriusmystery.htm

Thomson, W. (Lord Kelvin), 1881. The tide gauge, tidal harmonic analyzer, and tide predictor. Proceedings of the Institution of Civil Engineers 65, 3-24.

Tinsley, B. A., 2008. The global atmospheric electric circuit and its effects on cloud microphysics. Rep. Prog. Phys. 71, 066801.

Ulrych, T. J., and T. N. Bishop, 1975. Maximum entropy spectral analysis and autoregressive decomposition. Rev. Geophys. Space Phys. 13, 183-200.

Wang, Y.-M., J. L. Lean, and N. R. Sheeley, Jr., 2005. Modeling the Sun’s Magnetic Field and Irradiance since 1713. The Astrophys. J. 625, 522-538.

White, W. B., J. Lean, D. R. Cayan, and M. D. Dettinger, 1997. Response of global upper ocean temperature to changing solar irradiance. J. Geophys. Res. 102, 3255-3266.

Wild, M., 2009. Global dimming and brightening: A review. J. Geophys. Res. 114, D00D16, doi:10.1029/2008JD011470.

Willson, R. C., and A. V. Mordvinov, 2003. Secular total solar irradiance trend during solar cycles 21-23. Geophys. Res. Lett. 30, 1199-1202.

Wilson, R. M., 1987. On the Distribution of Sunspot Cycle Periods. J. Geophys. Res. 92, 10101-10104.

Wilson, I. R. G., B. D. Carter, and I. A. Waite, 2008. Does a spin-orbit coupling between the Sun and the jovian planets govern the solar cycle? Pub. of the Astr. Soc. of Astralia 25, 85-93.

Wolf, R., 1859. Extract of a letter to Mr. Carrington. Mon. Not. R. Astron. Soc. 19, 85-86.

Wolff, C. L., and P. N. Patrone, 2010. A New Way that Planets Can Affect the Sun. Solar Physics 266, 227-246.

Yadava, M. G., and R. Ramesh, 2007. Significant longer-term periodicities in the proxy record of the Indian monsoon rainfall, New Astronomy 12, 544555.

Yu, Z., S. Chang, M. Kumazawa, M. Furumoto and A. Yamamoto, 1983. Presence of periodicity in meteorite falls. National Institute of Polar Research, Memoirs, Special issue (ISSN 0386-0744), 30, 362-366.

Cycle	Temp/Fig4A	AAR	fig4B	fig4C	fig4D
#1	9.1 ± 0.2	9.15 ± 0.2	9.1 ± 0.2	9.2 ± 0.2	n/a
#2	10.4 ± 0.3	10.33 ± 0.3	10.0 ± 0.3	10.2 ± 0.3	10.8 ± 0.3
#3	20.9 ± 0.9	20.6 ± 0.9	21.3 ± 0.9	20.3 ± 0.9	20.2 ± 0.9
#4	32 ± 2	29.5 ± 2	29 ± 2	30 ± 2	n/a
#5	62 ± 5	62 ± 5	62 ± 5	64 ± 8	60 ± 5

Table 1: First column: periods of the cycles #1, #2, #3, #4 and #5 found in the global surface temperature: see Figure 4A. Third column: periods of the cycles #1, #2, #3, #4 and #5 found in the 1700-1966 aurora record: see Figure 4B. Fourth column: periods of the cycles #1, #2, #3, #4 and #5 found in the 1700-1880 aurora record: see Figure 4C. Fifth column: periods of the cycles #2, #3 and #5 found in the 1872-1966 aurora record: see Figure 4C. Second column: average of the periods of the cycles #1, #2, #3, #4 and #5 found in the three aurora records. The results depicted in the first and second column are perfectly coherent within the error of measure for each couple of values. For the 5 frequency couples combined, the reduced χ^2 is $\chi_o^2 = 0.18$ with 5 degrees of freedom ($P_5(\chi^2 \geq \chi_o^2) > 96\%$).

Group I	Jupiter Right asc.	Decl.	Dist	Saturn Right asc.	Decl.	Dist	tidal elong.
Jun 23, 2000	3h 19m 29.7s	17^o 19’ 48”	4.996	3h 20m 46.9s	16^o 09’ 35”	9.148	1801
Nov 15, 1940	2h 38m 22.5s	14^o 17’ 03”	4.975	2h 40m 02.0s	13^o 06’ 15”	9.206	1822
Apr 3, 1881	1h 59m 49.6s	10^o 56’ 01”	4.960	2h 01m 41.6s	9^o 46’ 24”	9.271	1836
Sep 16, 1821	1h 23m 54.9s	7^o 27’ 24”	4.951	1h 25m 41.6s	6^o 19’ 26”	9.339	1843
Feb 23, 1762	0h 50m 01.2s	3^o 56’ 49”	4.948	0h 51m 51.2s	2^o 53’ 04”	9.408	1846
Aug 8, 1702	0h 17m 53.7s	0^o 30’ 16”	4.949	0h 19m 43.3s	-0^o 28’ 12”	9.477	1843
$\sim$							
Mar 9, 1206	3h 38m 35.0s	18^o 45’ 16”	5.054	3h 39m 46.7s	17^o 39’ 14”	9.027	1747
Jul 26, 1146	2h 55m 26.0s	15^o 47’ 32”	5.023	2h 56m 58.1s	14^o 38’ 17”	9.064	1776
Dec 14, 1086	2h 14m 02.8s	12^o 20’ 48”	4.998	2h 15m 45.0s	11^o 10’ 10”	9.116	1800
Group II							
Apr 17, 1981	12h 28m 16.4s	-1^o 38’ 06”	5.451	12h 29m 57.6s	-0^o 38’ 21”	9.563	1395
Aug 23, 1921	11h 51m 01.8s	2^o 21’ 51”	5.442	11h 52m 34.2s	3^o 14’ 38”	9.476	1404
Dec 28, 1861	11h 13m 17.8s	6^o 20’ 14”	5.427	11h 14m 40.1s	7^o 04’ 21”	9.393	1418
May 8, 1802	10h 35m 26.9s	10^o 06’ 06”	5.405	10h 36m 27.1s	10^o 41’ 21”	9.314	1436
Sep 18, 1742	9h 57m 07.1s	13^o 33’ 53”	5.378	9h 57m 49.9s	13^o 58’ 48”	9.241	1458
Feb 2, 1683	9h 18m 23.2s	16^o 36’ 37”	5.347	9h 18m 43.6s	16^o 50’ 56”	9.177	1484
Group III							
Apr 16, 1960	19h 42m 18.9s	-21^o 40’ 29”	5.146	19h 42m 10.4s	-21^o 23’ 03”	10.028	1635
Sep 28, 1901	19h 07m 48.3s	-22^o 40’ 42”	5.177	19h 07m 38.6s	-22^o 13’ 36”	10.053	1607
Mar 12, 1842	18h 33m 28.3s	-23^o 12’ 38”	5.207	18h 33m 23.7s	-22^o 36’ 25”	10.072	1580
Aug 26, 1782	17h 59m 51.0s	-23^o 16’ 44”	5.236	17h 59m 50.7s	-22^o 32’ 18”	10.082	1555
Feb 11, 1723	17h 26m 46.3s	-22^o 54’ 28”	5.264	17h 27m 03.5s	-22^o 02’ 54”	10.086	1531
Jul 31, 1663	16h 54m 47.2s	-22^o 08’ 09”	5.291	16h 55m 15.1s	-21^o 10’ 25”	10.083	1509

Table 2: Approximates dates of the J/S conjunctions relative to the Sun, which slightly differ from the conjunction dates as relative to the Earth. The coordinate of the planets are in Right Ascension and Declination in heliocentric equatorial coordinates which are relative to the equatorial plane of the Earth. The last column report the approximate value of the tidal elongation in Km (see Eq. 2) at the orbit of the Earth, that is, at 1 AU from the Sun.

	$P_1(t)$ (1850-2009)	$P_1(t)$ (1950-2009)	$P_2(t)$ (1850-1950)
a	0.103 ± 0.011	0.109 ± 0.018	0.098 ± 0.015
b	0.022 ± 0.011	0.031 ± 0.018	0.020 ± 0.015
c	0.040 ± 0.011	0.043 ± 0.018	0.036 ± 0.015
d	0.027 ± 0.011	0.030 ± 0.018	0.027 ± 0.015
e	-0.053 ± 0.011	-0.055 ± 0.018	-0.050 ± 0.015
f	-0.006 ± 0.008	-0.024 ± 0.013	-0.006 ± 0.010
α	2.08 ± 0.5	1.84 ± 0.6	2.41 ± 0.7
β	1.43 ± 0.4	1.81 ± 0.6	1.14 ± 0.6
γ	-0.32 ± 0.2	-0.47 ± 0.3	-0.26 ± 0.3

Table 3: Multi nonlinear regression coefficients to fit of the global surface temperature record using the functions $P_1(t)$ and $P_2(t)$. $P_1(t)$ is used to fit two periods: 1850-2009 and 1950-2009. $P_2(t)$ is used to fit the period 1850-1950. Note that the three sets of coefficients coincide within the errors of measure. Thus, there exists an accurate statistical coherence between the three models. For the 9 coefficient couples relative to the independent results reported in the last two columns the reduced χ^2 is $\chi_o^2 = 0.34$ with 9 degrees of freedom ($P_9(\chi^2 \geq \chi_o^2) > 95\%$).